Nuclear Engineering and Technology 53 (2021) 2104–2125

Contents lists available at ScienceDirect

Nuclear Engineering and Technology

journal homepage: www.elsevier.com/locate/net

Original Article

Verification and validation of isotope inventory prediction for back-end cycle management using two-step method

Jaerim Jang, Bamidele Ebiwonjumi, Wonkyeong Kim, Alexey Cherezov, Jinsu Park, Deokjung Lee*

Department of Nuclear Engineering, Ulsan National Institute of Science and Technology, 50 UNIST-gil, Ulsan, 44919, Republic of Korea

ARTICLE INFO

Article history:
Received 23 February 2020
Received in revised form
17 September 2020
Accepted 7 January 2021
Available online 15 January 2021

Keywords:
PWR
Isotope inventory
Isotope inventory prediction
Back-end cycle

ABSTRACT

This paper presents the verification and validation (V&V) of a calculation module for isotope inventory prediction to control the back-end cycle of spent nuclear fuel (SNF). The calculation method presented herein was implemented in a two-step code system of a lattice code STREAM and a nodal diffusion code RAST-K. STREAM generates a cross section and provides the number density information using branch/history depletion branch calculations, whereas RAST-K supplies the power history and three history indices (boron concentration, moderator temperature, and fuel temperature). As its primary feature, this method can directly consider three-dimensional core simulation conditions using history indices of the operating conditions. Therefore, this method reduces the computation time by avoiding a recalculation of the fuel depletion. The module for isotope inventory calculates the number densities using the Lagrange interpolation method and power history correction factors, which are applied to correct the effects of the decay and fission products generated at different power levels. To assess the reliability of the developed code system for back-end cycle analysis, validation study was performed with 58 measured samples of pressurized water reactor (PWR) SNF, and code-to-code comparison was conducted with STREAM-SNF, HELIOS-1.6 and SCALE 5.1. The V&V results presented that the developed code system can provide reasonable results with comparable confidence intervals. As a result, this paper successfully demonstrates that the isotope inventory prediction code system can be used for spent nuclear fuel analysis.

1. Introduction

This paper presents the verification and validation of a module used to predict the isotope inventory for spent nuclear fuel (SNF) and its application in the Westinghouse 2-loop pressurized water reactor (PWR), which is one of the power plant types used in South Korea. The target reactor has 2,904 calculation nodes per cycle: 121 radial nodes (*i.e.*, the number of fuel assemblies) and 24 axial nodes per assembly for nodal calculation. An in-house code, STREAM-SNF, was previously developed for an analysis of the isotope inventory and can provide results with up to 7% accuracy as compared with the Takahama-3, Calvert Cliffs-1, and GKN II benchmark problems [1]. The total simulation time of the SNF analysis was 30.25 (15 min/node × 2,904 calculation nodes) days per cycle, as calculated using STREAM-SNF, where the calculation time for one fuel node was approximately 15 min using a single processor. If the core simulates N cycles, it requires 30.25 × N days. To reduce the simulation time, the SNF module was developed using a two-step code system. A Lagrange interpolation, with a history index of the core simulation, was adopted to reduce the number of re-calculations of the depletion after a three-dimensional (3D) core simulation.

Because the spent fuel pools of Kori units 1–4 will become fully saturated by 2024 [7], the management of the spent fuel assembly is an important issue in South Korea. To ensure safety in the management and transport of SNF, an SNF inventory calculation is important for predicting the decay heat, radiological response activity, and neutron/gamma source strengths. Furthermore, this calculation is required for radiation shielding and SNF cask analysis [2–4], burnup credit criticality analysis [5], and management of radioactive wastes (evaluation of expected masses and the cost of waste disposal) [6]. An SNF analysis module is therefore implemented. In this study, we employed 58 measured samples of PWR SNF to validate the isotope inventory prediction capability of the SNF analysis module. The measurement data used comes from 15

* Corresponding author.
E-mail address: deokjung@unist.ac.kr (D. Lee).

https://doi.org/10.1016/j.net.2021.01.009

different fuel pins and five different PWRs: Takahama-3, Calvert Cliffs-1, Turkey Point-3, Three Mile Island (TMI)-1, and Obrigheim. These are described in detail in Section 3.1 and summarized in Table 1. We would like to mention that the SNF analysis module implemented in this study can calculate the isotope inventory, radioactivity, decay heat, neutron and gamma source strengths/spectra of irradiated fuel. In other words, it encompasses the SNF radiation source terms. However, only the isotope inventory calculation results are verified and validated. V&V of the decay heat calculations results can be found in the reference [12]. The remainder of this paper is arranged as follows: Section 2 describes the STREAM/RAST-K code system which contains the implementation of the isotope inventory prediction module. Section 3 describes the measurement data and details the verification and validation results. The conclusion and future work are presented in Section 4.

2. Description of two-step code system

In this section, the two-step code system, a lattice code STREAM, and a nodal code RAST-K v2.0, used for the SNF analysis is described. STREAM is a transport code that creates cross sections using a pointwise energy slowing-down method and a two-dimensional (2D) form function with a reflective boundary [8,9]. STREAM-SNF was developed to analyze the back-end cycle fuel assembly and was validated based on various benchmark problems. Three reactor types were used for the validation of the isotope inventory prediction, the errors of which were within the range of −7% to +7%; in addition, 91 decay heat samples were employed for validation, the errors of which were within 5%. Therefore, STREAM-SNF was employed for a code-to-code comparison, and the ENDF/B-VII.0 library was used to maintain consistency with the previous validation of the STREAM-SNF module [1,8–10].

The previous analysis of the predicted isotope inventory was conducted in four steps: 1) calculation of the cross section using the lattice code STREAM, 2) a core calculation using the nodal code RAST-K, 3) a depletion calculation of STREAM using the historical conditions generated through a 3D core calculation, and 4) cooling of the assays [11,12]. The calculation system developed in this work can be used to reduce the calculation time and avoid a recalculation of the depletion in step 3.

RAST-K 2.0 is a nodal diffusion code applying a 3D multigroup unified nodal method and a multigroup coarse mesh finite difference acceleration [14–16]. An inventory of 36 isotopes was generated by heavy nuclide and fission product depletion chains, which is made up of 22 actinides, 12 fission products, and 2 burnable position isotopes (gadolinium). A simplified 1D single-channel thermal-hydraulic (TH1D) solver was implemented in RAST-K 2.0 to correct the cross sections with thermal-hydraulic feedback [14–16]. However, to maintain consistency in the validation when applying the STREAM-SNF module and to consider the fixed-temperature conditions presented in the reference [13], the TH1D solver was not used in the realistic benchmark calculation.

Fig. 1 shows the code system workflow of the source-term calculation implementation. During the RAST-K core-following operation, three history indices are generated: (1) the boron concentration (BOR), (2) fuel temperature (TFU) and (3) moderator temperature (TMO). The number densities of 1,640 isotopes are calculated using the Lagrange interpolation method with the history indices [16]. History depletion branch cases are presented in detail in the reference [12]. A total of 10 history cases are used for the interpolation. The number density is calculated using the Lagrange interpolation through Equation (1) [12].

$$ND_{calculate} = ND_{BASE} + \Delta ND_{TMO} + \Delta ND_{TFU} + \Delta ND_{BOR}, \quad (1)$$

where $ND_{calculate}$ is the number density calculated using the Lagrange interpolation [12,17], ND_{BASE} is the number density calculated using the main branch, and ΔND is the difference in number density caused by the different calculation conditions (*i.e.*, between the history index and the main branch condition). Equation (2) shows the definition of the history index and the application of the Lagrange interpolation. The history index is calculated using the time-average value of the three conditions, *i.e.*, boron concentration, moderator temperature, and fuel temperature.

$$\Delta ND = ND(h) - ND_{BASE} = \sum_{i=1}^{N}(L_i(h)ND_i)$$
$$- ND_{BASE} = \sum_{i=1}^{N}\left(L_i\left(\frac{\sum_{i=1}^{n} x_i \Delta t_i}{\sum_{i=1}^{n} \Delta t_i}\right)ND_i\right) - ND_{BASE}, \quad (2)$$

where i is the index, L_i is the Lagrange coefficient, h is the history index, x is the parameter (*e.g.*, TMO, TFU, and BOR), N is the number of history depletion branches (five for TMO, three for TFU, and four for BOR), and n is the number of burnup steps. Detailed equations of the Lagrange interpolation used in this study are shown in the reference [12]. Equation (3) is the corrected result using a power correction factor [18]. The power correction factor was derived from the linear decay chain equation [18,19], and was adopted to consider the decay effect between different power levels [18].

$$ND_{corrected} = ND_{calculate} * PCF, \quad (3)$$

where $ND_{corrected}$ is the final result of the isotope inventory prediction, and PCF is the power correction factor, which depends on the differences in the power and flux between the 2D branch calculation and the 3D core simulation [18]. The base files of the number density for interpolation are generated through a STREAM 2D fuel assembly (FA) history depletion branch calculation with a reflective boundary.

Table 1
Specifications of validation cases.

Reactor	Measurement facility	Assembly Design	Enrichment (wt.% ^{235}U)	Burnup [GWd/MTU]	No. of M/P[a]	Decay Time [years]
Takahama-3	JAERI	17 × 17	4.11	14.3–47.25	10/2	3.96 (Sm[b])
Calvert Cliffs-1	KRI[c], PNL[d]	14 × 14	2.72, 3.038	18.68–44.34	6/2	6.504–12.76
Turkey Point-3	Battelle-Columbus	15 × 15	2.556	30.51–31.56	5/2	2.540
TMI-1	ANL[e], GE-VNC[f]	15 × 15	4.013, 4.657	22.8–55.7	19/4	3.022–4.688
Obrigheim	JRC[g] Ispra, Karlsruhe	14 × 14	2.83, 3.00	17.13–37.49	18/5	

a is M/P: Measurements/pins; *b* means that only samarium isotope was measured after the cooling period; *c* is Khlopin Radium Institute (KRI); *d* is Pacific Northwest National Laboratory (PNL); *e* is Argonne National Laboratory (ANL); *f* is General Electric Vallecitos Nuclear Center (GE-VNC); *g* is Joint Research Center, European Commission (JRC).

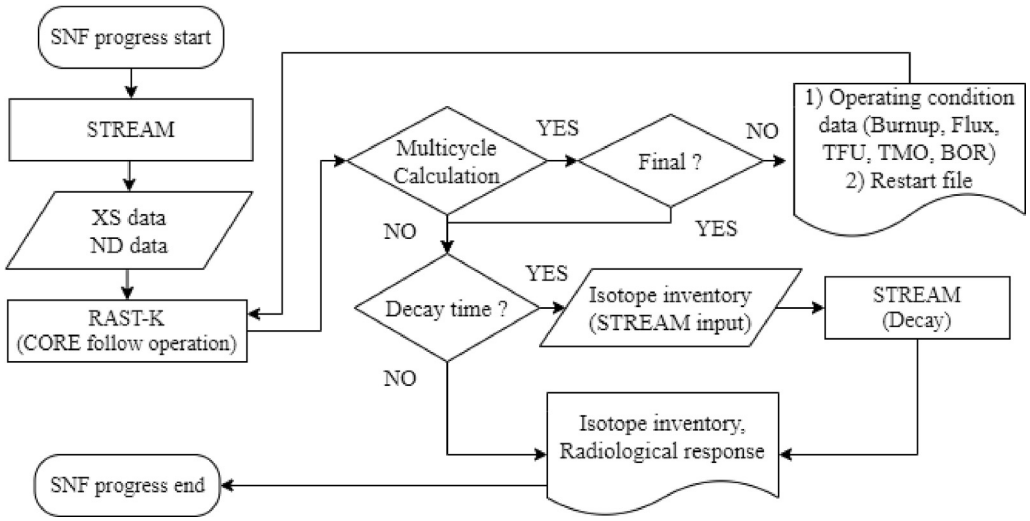

Fig. 1. Flow chart of source-term calculation using two-step method.

After the calculation of the isotope inventory, the source terms (decay heat, radiological response activity, and neutron/gamma source strengths) can be calculated using two methods, *i.e.*, the RAST-K and STREAM source-term calculation modules. When the STREAM source-term calculation module is used, RAST-K generates the isotope inventory. The difference between the two approaches is the treatment of the cooling period after discharge. During a cooling calculation, the RAST-K source term module is not used. RAST-K is used to predict the isotope inventory which is used in the STREAM cooling and source term calculations.

3. Verification and validation results using benchmark problems

3.1. Description of measurement data

This section presents the details of realistic benchmark assays used to validate the isotope inventory prediction module. Table 1 shows the initial enrichment, discharged burnup, decay time (*i.e.*, cooling time), number of pins and measurements, and measurement facilities. The ranges of the initial enrichment and burnup are 2.556–4.657 wt% and 14.3–55.7 GWd/MTU, respectively.

The Takahama-3 PWR, operated in Japan by Mitsubishi Nuclear Fuel and Nuclear Fuel Industries, uses 17 × 17 fuel assemblies [14]. The Takahama-3 samples were measured at the Japan Atomic Energy Research Institute (JAERI). For these samples, the samarium isotope was measured after a cooling time of 3.96 years. Calvert Cliffs-1, Turkey Point-3, and TMI-1 are PWRs operated in the United States and these reactors provided a total of 30 measured SNF samples from 8 different pins for validation. The Obrigheim PWR operated in Germany, and for validation, 18 measured SNF samples obtained from 5 fuel pins in this reactor are used. Fig. 2 shows the radial layout of the FAs from which the fuel rods and measured samples are obtained [14]. This figure also shows the location of the fuel rods which contain the measured samples. All measured fuel pins use UO_2 fuel without a burnable absorber (*i.e.*, pin type 1). The operating conditions include the boron concentration, moderator temperature, fuel temperature, specific power density, operating periods, and overhaul periods and are presented in detail in the reference [14].

3.2. Verification and validation using Takahama-3 measurements

This section presents the verification and validation results for the Takahama-3 FA. Takahama-3 is a PWR in Japan, and JAERI measured 16 samples from three fuel rods in FAs with IDs NT3G23 and NT3G24 [14]. In this study, however, 10 samples from two fuel rods are considered and the calculation-to-experiment ratio (C/E) comparison results are presented. Because STREAM-SNF is used for code-to-code comparison, 10 samples from a previous validation study on STREAM-SNF are selected [1]. Fig. 3 shows the axial and radial layout of the FA containing the measured fuel rods. Five samples are obtained from the SF95 pin, as shown in subplot (b) of Fig. 3. A height of 0 cm indicates the bottom of the fuel rod, where the active height is 366 cm. Table 2 shows the design specifications of the Takahama-3 FA [1,11,12,14,20]. The operating conditions of the samples are described in document [14]. The SF95 pin was from a twice-burned NT3G23 FA (having undergone cycle 5 and 6 operations), and assays of the SF97 pin are from a thrice-burned NT3G24 FA (having undergone cycle 5, 6, and 7 operations). For the calculation, the samples are built as pin models with reflective boundaries, and overhaul periods are considered.

In the appendix, Table A. 1 shows the comparison results with 10 measurements using STREAM-SNF and RAST-K SNF. A total of 20 axial nodes were used for the nodal calculations (each of which was 18.3 cm in height). The value of σ_C is the standard deviation of the C/E distribution, and σ_M is the standard deviation of the measurement, as presented in the reference [14]. The calculation results are first converted to the ratio of calculated mass per initial uranium mass (g/gU_{init}) before comparison with measured data. Samarium isotope was measured after a cooling period of 3.96 years. Most isotopes demonstrated a similar scale error compared to the validated STREAM-SNF. Fig. 4 shows a comparison between the calculation results of RAST-K SNF and the measurements, and Fig. 5 provides the average results ($\overline{C/E}$) of the STREAM-SNF and RAST-K SNF calculations. These figures are for the samples from the SF95 fuel rod. In addition, Fig. 6 shows the absolute and relative differences compared with the experimental data in the SF95-1 sample. The nuclides: ^{242m}Am, ^{243}Cm, and ^{245}Cm have the largest relative errors. By contrast, these isotopes have the smallest absolute differences of approximately 0.01 $g/g_{initial\ U}$. Fig. 7 shows the depletion chain used for the micro-depletion in RAST-K. A sensitivity study is conducted with −1% change in the initial mass of ^{238}U. The values

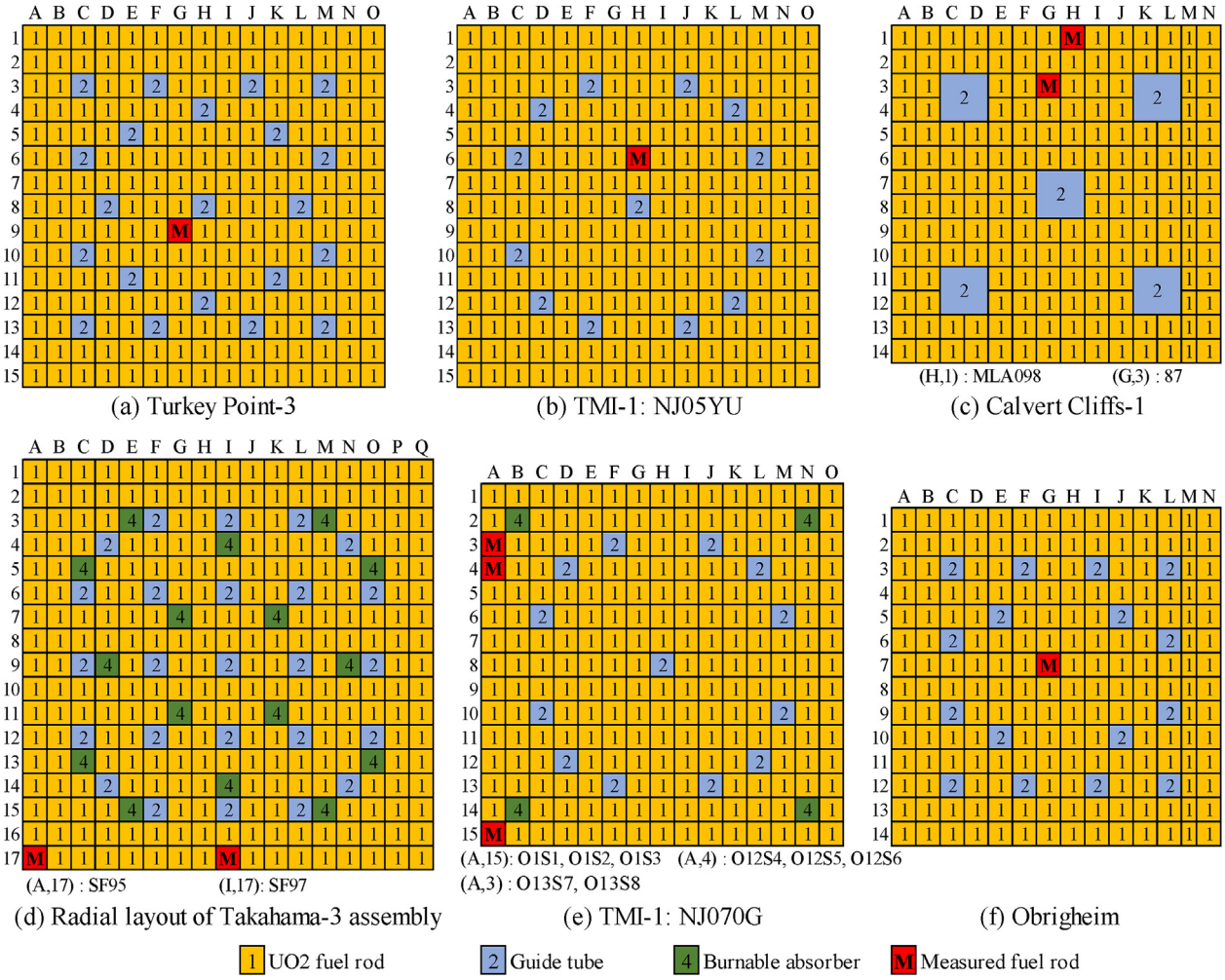

Fig. 2. Radial layout of fuel assemblies.

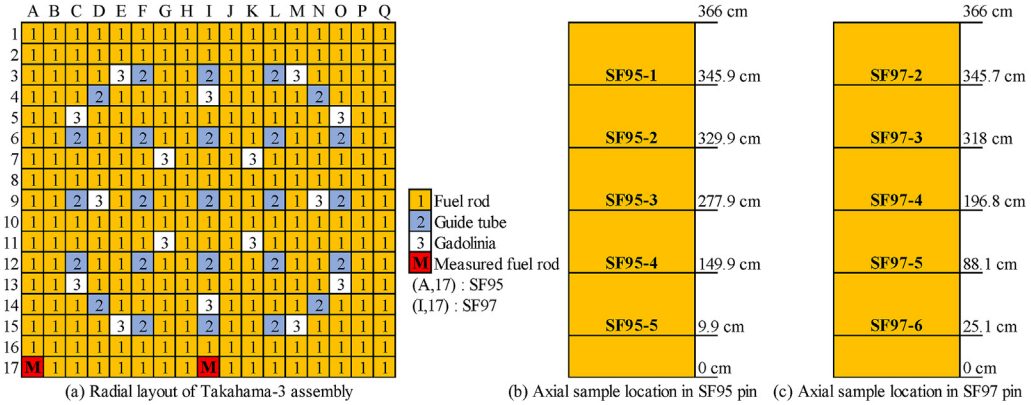

Fig. 3. Layout of Takahama-3 FA

in blue indicate the relative difference in mass ratio ($g/g_{initial\ U}$) according to the change in the initial concentration of ^{238}U. The amount of ^{242m}Am is decreased by 1%, whereas those of ^{242}Am, ^{242}Cm, and ^{243}Cm decrease by 2.03%, 2.05%, and 3.06%, respectively. From Figs. 4 and 6, it can be seen that the mass of ^{238}U affects the amounts of ^{242}Cm and ^{243}Cm.

As indicated in Fig. 5, the relative difference in ^{245}Cm is large. Fig. 8 shows the decay chain of ^{245}Cm and ^{246}Cm. These nuclides are calculated using a Lagrange interpolation method based on the discharge burnup, boron concentration, moderator temperature, and fuel temperature. Because the benchmark burnup reported in document [14] was calculated using the standard ASTME 321-79 method with an uncertainty of up to 3% [1], the sensitivity study was conducted under the discharge burnup conditions to indicate

Table 2
Fuel design specifications of Takahama-3 FA.

Parameter	Value	Unit
Number of measured FAs	2 (SF95, SF97)	
Number of measured pins	10	
Rod pitch[a]	1.311	cm
Radius of fuel pin	0.4025	cm
FA type	17 × 17	
Radius of inner cladding	0.4110	cm
Radius of outer cladding	0.4750	cm
Enrichment of ^{235}U	4.11 (SF95) 2.63 (SF97)	wt.%
Average fuel rod temperature	900	K
Active fuel rod height	366	cm

[a] Equivalent cell pitch for each measured fuel rod [1].

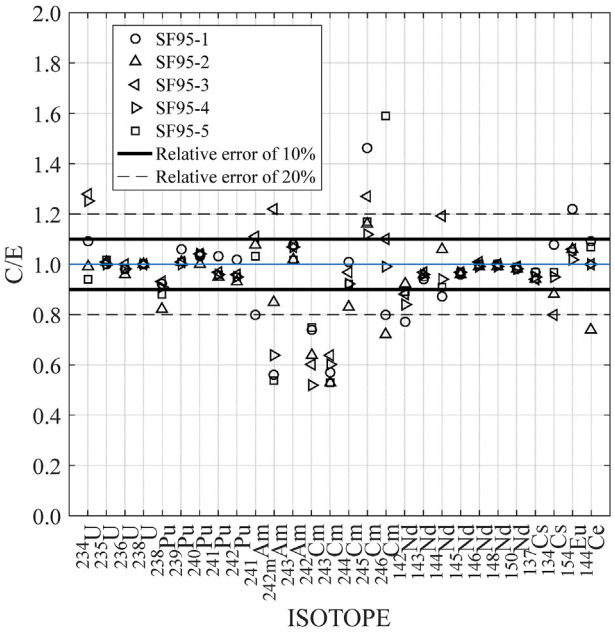

Fig. 4. RAST-K SNF ratio of calculated-to-measured (C/E) isotope inventories of SF95 fuel samples.

the difference according to an uncertainty of the design parameters [21]. The nuclides of ^{245}Cm and ^{246}Cm show changes of −6.21% and −8.17% as the discharge burnup is changed by −1%. The uncertainty of the burnup conditions can affect the ^{245}Cm and ^{246}Cm.

Fig. 9 shows the relative errors of the SF97 samples discharged from Takahama-3. Most of the isotopes are within the ±20% error boundary. In addition, Fig. 10 shows the mean ratio of the calculated and measured results, and Fig. 11 provides the mass ratio as compared with the measurements. The nuclides of ^{242m}Am, ^{243}Cm, and ^{149}Sm have large relative errors similar with the SF95 samples.

3.3. Verification and validation results

This section presents the verification and validation results of the 58 measured samples from five different reactors: Takahama-3, Calvert Cliffs-1, Turkey Point-3, TMI-1, and Obrigheim. The Appendix contains the relative errors (C/E−1 [%]) of 26 nuclides: ^{234}U, ^{235}U, ^{236}U, ^{238}U, ^{238}Pu, ^{239}Pu, ^{240}Pu, ^{241}Pu, ^{242}Pu, ^{237}Np, ^{241}Am, ^{242m}Am, ^{243}Am, ^{95}Mo, ^{99}Tc, ^{101}Ru, ^{103}Rh, ^{143}Nd, ^{145}Nd, ^{147}Sm, ^{149}Sm, ^{150}Sm, ^{151}Sm, ^{152}Sm, ^{151}Eu, and ^{153}Eu. Fig. 12 shows the mean ratio of the calculated and measured results. STREAM-SNF was used as a reference in a code-to-code comparison. Tables A. 2 and A. 3 in the

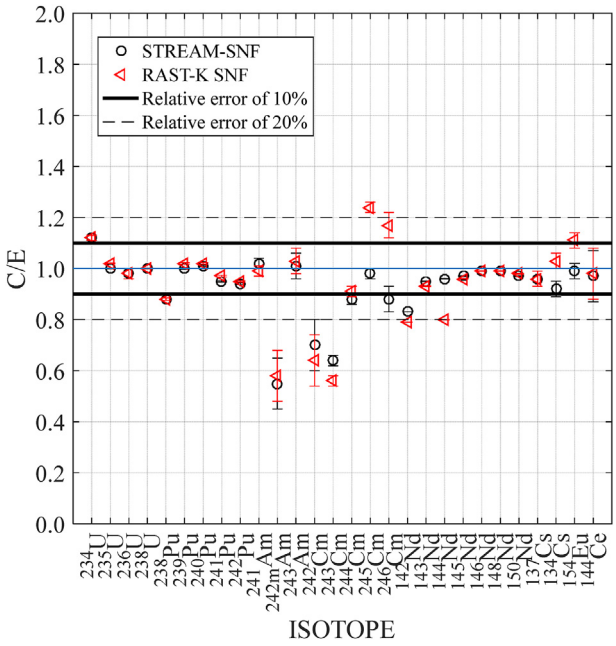

Fig. 5. Mean calculated-to-measured ratio (C/E) for SF95 fuel samples.

appendix contain the detail mean ratio of STREAM-SNF and RAST-K SNF and the average relative difference between the STREAM-SNF and RAST-K SNF calculation results. The nuclides of ^{242m}Am and the curium isotopes show a large difference compared with the STREAM-SNF results, whereas the trends of $\overline{C/E}$ are similar.

The isotopes of ^{242m}Am, ^{242}Cm, ^{243}Cm, and ^{247}Cm are underestimated compared with the measurements. The ^{245}Cm results are overestimated. The ^{242m}Am isotope is generated by a capture reaction with ^{241}Am, and is lost from an isometric transition and an α decay rection with ^{242}Am and ^{238}Np, respectively [15]. Because ^{242m}Am is underestimated by 22%, it can be seen that the lost reactions have a dominant effect on the amount of ^{242m}Am. The underestimation of ^{242m}Am influences the underestimation of ^{242}Am as an isometric transition, and the 12% underestimation of ^{242}Cm is affected by the underestimation of ^{242}Am through a β^- decay reaction. Considering the 12% underestimation of the nuclide of ^{242}Cm, as shown in Table A. 2, ^{242}Cm may result in a 22% underestimation of ^{243}Cm through a capture cross section. Fig. 7 deals with micro-depletion for 13 isotopes and more detail information is describe in document [15].

The ^{245}Cm is generated by ^{245}Am (β^- decay), ^{249}Cf (α decay), and ^{244}Cm (n, γ). The overestimation of ^{244}Cm can affect the overestimation of ^{245}Cm. In addition, ^{247}Cm is generated by ^{247}Am (β^- decay), ^{251}Cf (α decay), and ^{246}Cm (n, γ). Therefore, the underestimation of ^{246}Cm can affect the underestimation of ^{247}Cm. Moreover, to consider the calculation uncertainty caused by the cross-section library, the relative errors in the curium isotopes can be within two standard deviations. In the reference [22], the authors describe the calculation uncertainty caused by the ENDF/B-VII.1 cross-section library for two samples of the LWR-PROTEUS II program. The isotopes of ^{246}Cm, ^{245}Cm, and ^{243}Cm have uncertainties of 29.79%, 16.38%, and 12.84%, respectively [22]. To consider such uncertainty, the relative error of ^{246}Cm is within one standard deviation, whereas ^{245}Cm and ^{243}Cm are within two standard deviations. However, because these uncertainties in the isotopes are generated by ENDF/B-VII.1, a quantification of the uncertainty will be determined using ENDF/B-VII.0 for the 58 measured samples in a future study.

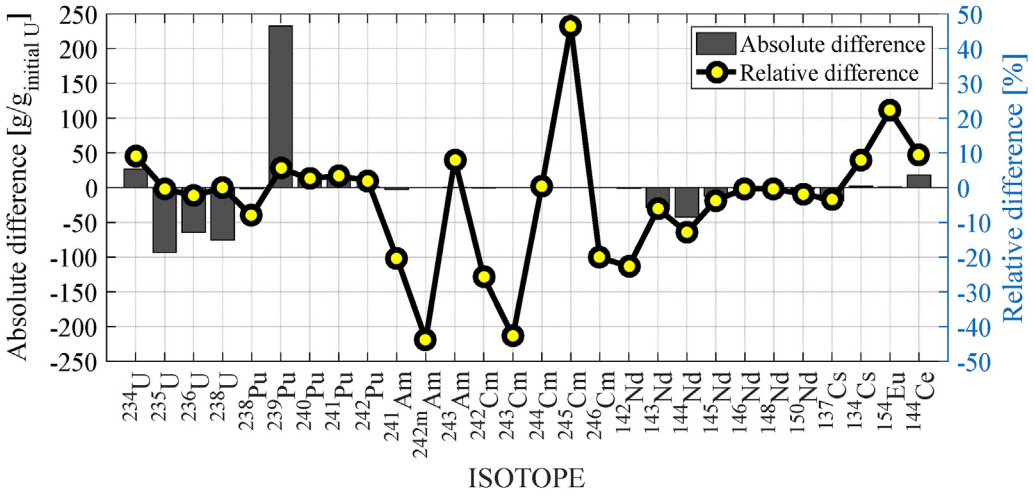

Fig. 6. Absolute difference ($g/g_{initial\ uranium}$) and relative difference for isotopes of SF95-1 sample.

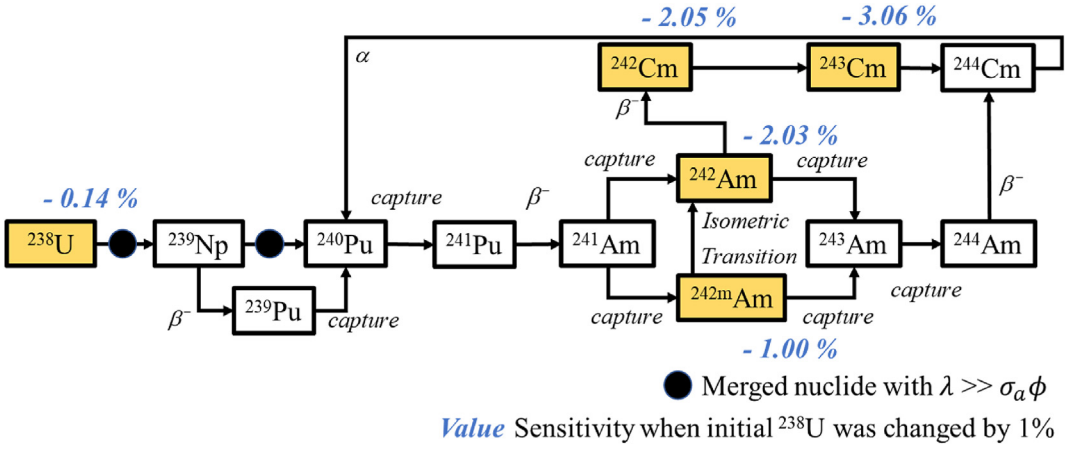

Fig. 7. Depletion chain with initial amount of change in uranium (RAST-K).

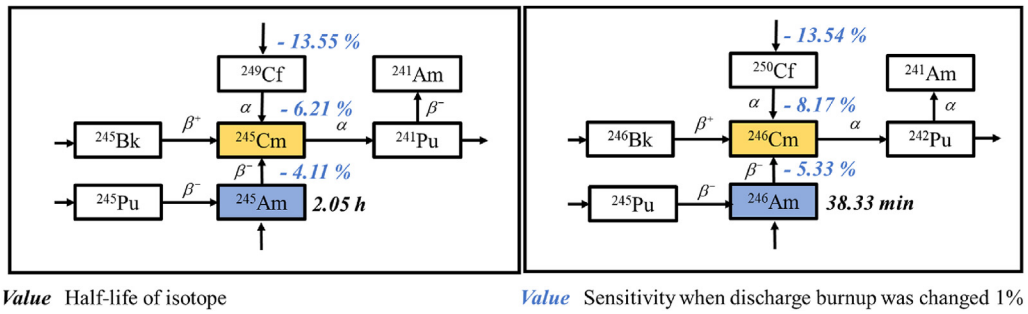

Fig. 8. Decay chain of ^{245}Cm and ^{246}Cm.

The mean of the results calculated for the 58 measured samples are shown in Fig. 12. The ^{245}Cm has a much larger relative error than that of the other isotopes. Fig. 13 shows the mean ratio of each of the five different reactors. The ^{245}Cm content of the NJ070G pin samples discharged from TMI-1 show large relative errors. The average relative differences are within ±4% for the actinides ^{234}U, ^{235}U, ^{236}U, ^{238}U, ^{238}Pu, ^{240}Pu, ^{242}Pu, and ^{237}Np and fission products ^{95}Mo, ^{101}Ru, ^{103}Ru, ^{143}Nd, ^{144}Nd, ^{145}Nd, ^{146}Nd, ^{148}Nd, ^{150}Nd, ^{147}Sm, ^{150}Sm, ^{152}Sm, ^{154}Sm, ^{133}Cs, ^{135}Cs, ^{137}Cs, ^{144}Ce, ^{153}Eu, ^{90}Sr. In addition, average relative differences are within ±12% for ^{241}Am, ^{242}Cm, ^{244}Cm, and ^{246}Cm which are used in shielding analysis [2].

3.4. Error trend analysis

An error trend analysis was conducted to indicate the relationship between the parameters and the calculated-to-measured (C/E) ratio of the isotope inventories. Four parameters are tested, namely, the enrichment, decay time, burnup, and axial location of the

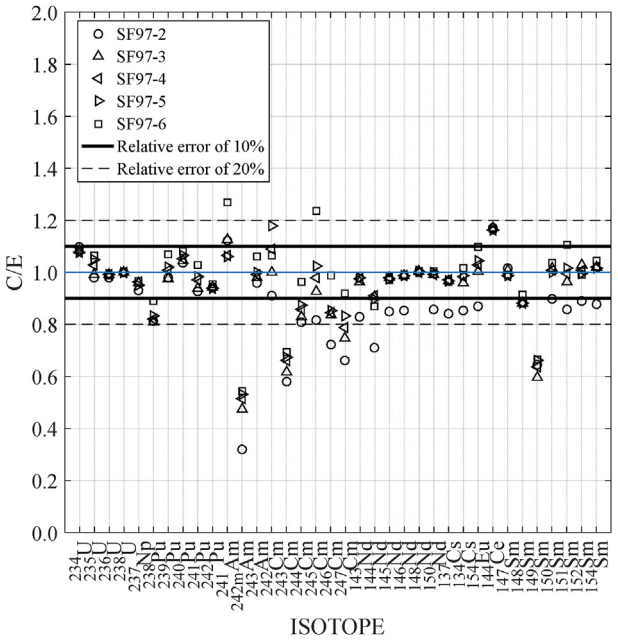

Fig. 9. RAST-K SNF ratio of calculated-to-measured (C/E) isotope inventories of SF97 fuel samples.

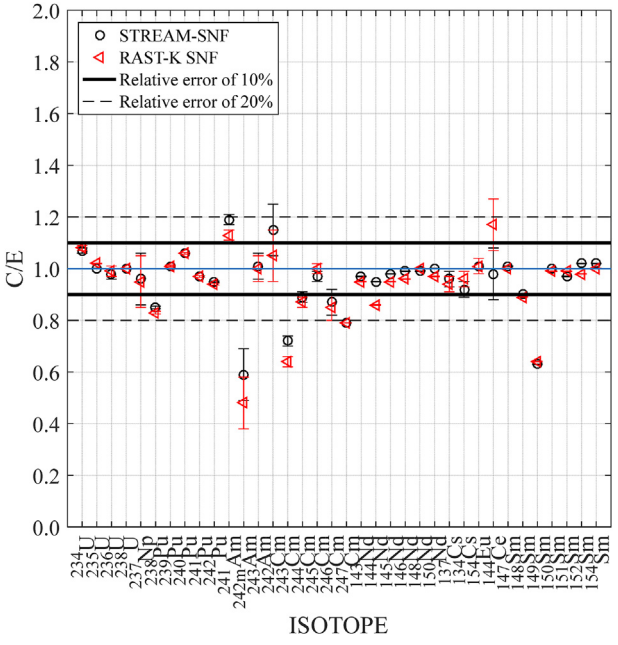

Fig. 10. Mean of calculated-to-measured ratio (C/E) for SF97 fuel samples.

samples. Detail specification of 58 samples are described in Ref. [14]. A total of 58 samples are used for the analysis. The ranges of samples axial location, rod pitch, enrichment, cooling period, and burnup are from 9.9 to 245.9 cm, 1.311–1.473 cm, 2.556–4.657 wt%, 2.54–12.76 years, and 14.3–55.7 MWd/kg, respectively.

Four isotopes with large relative differences are first examined: ^{242m}Am, ^{243}Cm, ^{244}Cm, and ^{245}Cm. The ratio of calculated-to-measured isotope inventories and their trend graphs are provided in Fig. 14. Detail trend analysis results are presented in Table A. 4. The trend of ^{245}Cm has a large slope in terms of enrichment, burnup, and cooling time. The linear-correlation coefficients of ^{245}Cm for the enrichment, discharge burnup, and cooling time are 0.3665, 0.2688, and 0.2345, as shown in Table A. 4. Linear-correlation coefficient is calculated following the reference [23] and the trend is calculated by least-square method [24]. Compared with the other three isotopes, the nuclide of ^{245}Cm has a stronger correlation with the design parameters. This indicates that ^{245}Cm has a large sensitivity according to the design parameters. In addition, Fig. 8 shows the relationship between the relative errors of ^{245}Cm and the discharge burnup. As indicated in the graph, ^{245}Cm changes by −6% according to a −1% change in the discharge burnup. In the cases of ^{242m}Am and ^{242}Cm, the effect of the cooling time is larger than that of the other parameters. The nuclide of ^{244}Cm has a smaller correlation with the parameters as compared with the other nuclides.

Fig. 15 shows the error trends of ^{234}U, ^{238}U, ^{238}Pu, and ^{240}Pu, which have smaller relative errors compared with the isotopes shown in Fig. 14. Table A. 5 lists the linear-correlation factors of uranium and plutonium isotopes. The linear-correlation coefficient is also smaller compared with that in Table A. 4. The nuclides of ^{234}U and ^{238}Pu have large correlations with the cooling time at 0.2325 and 0.2179, respectively.

3.5. Verification based on HELIOS-1.6 and SCALE5.1

To indicate the effect of the modeling parameters and libraries, this section describes the verification of the results based on the development of other spent fuel analysis code systems. Two codes are employed for the comparison: HELIOS-1.6 and SCALE5.1 [14,25]. HELIOS-1.6 has been validated with 16 samples (*i.e.*, SF95-1 to 5, SF96-1 to 5, and SF97-1 to 6) discharged from Takahama-3 [25], and these validation benchmark set includes the ten samples used in this study. In addition, SCALE5.1 calculation module has been validated against 119 spent nuclear fuel samples from PWRs, as shown in Ref. [14]. The spent fuel samples have a range of ^{235}U enrichment from 2.453 to 4.657 wt% and discharged burnups from 7.2 GWd/MTU to 70.4 GWd/MTU. The 119 spent fuel samples include the 58 measured samples calculated in this study. For calculation, HELIOS-1.6, SCALE 5.1, and RAST-K SNF use the ENDF/B-VI.0, ENDF/B–V.0, and ENDF/B-VI.8 library, respectively [14,25]. For the depletion calculations, HELIOS-1.6 and SCALE 5.1 use the FA model. RAST-K SNF uses the pin-cell model.

The HELIOS-1.6 (with 2D calculations) code package uses three programs, AURORA, HELIOS, and ZENITH. AURORA is used for defining the benchmark parameters (geometry, material composition, and calculation parameters) [25]. ZENITH saves the output data from HELIOS-1.6 and converts the data from a binary format into the ASCII format [25]. A quarter symmetric layout is applied in the FA calculation. In addition, HELIOS-1.6 considers the influence of the surrounding FA on the isotopic concentration of the samples because the measured samples are located at the outer edge of the FA [25]. Moreover, SCALE 5.1 code package uses the TRITON/NEWT depletion module to solve the 2D transport equation, and uses the 44 group ENDF/B–V.0 library [26].

The comparison results (C/E) are presented in Figs. 16–21. Figs. 16–21 present the ratio of calculated-to-measured nuclide content for samples discharged from Takahama-3, Calvert Cliffs-1, Turkey Point-3, TMI-1, and Obrigheim, respectively. These figures display the root mean square (RMS) of C/E as a function of burnup, and the detail C/E of some selected nuclides from some reactor samples. The nuclide C/E plot correspond to discharge burnup. The error bars on the calculated-to-measured ratios refer to one standard deviation of measurement [14].

As shown in section 3.4, Cm and Am isotopes have more strong relationship with discharge burnup condition compared with other parameters. Therefore, to assess the effect of burnup on C/E, C/E of

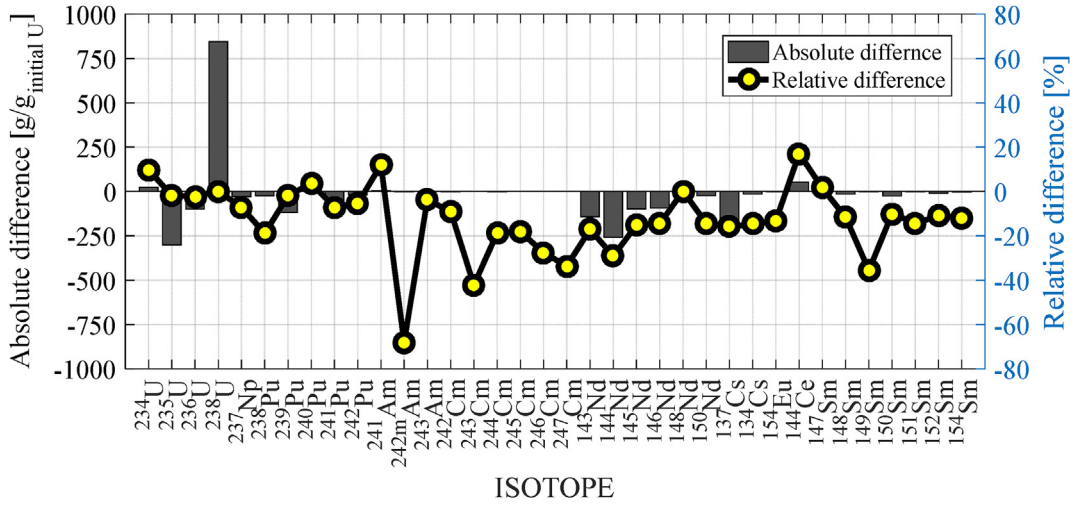

Fig. 11. Absolute difference ($g/g_{initial\ uranium}$) and relative difference for isotopes of SF97-2 sample.

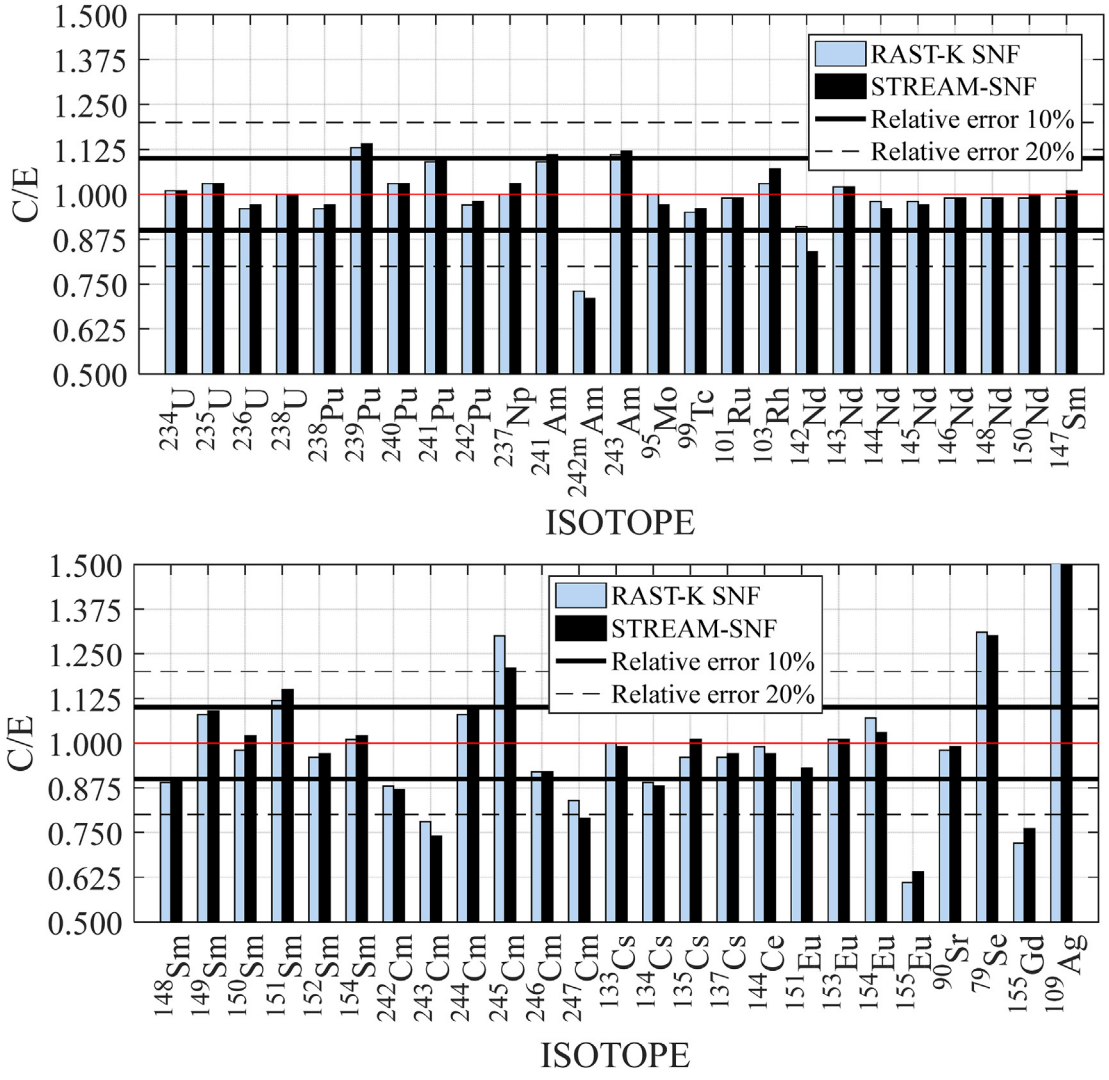

Fig. 12. Mean ratio of calculated-to-measured isotope inventories of STREAM-SNF and RAST-K SNF.

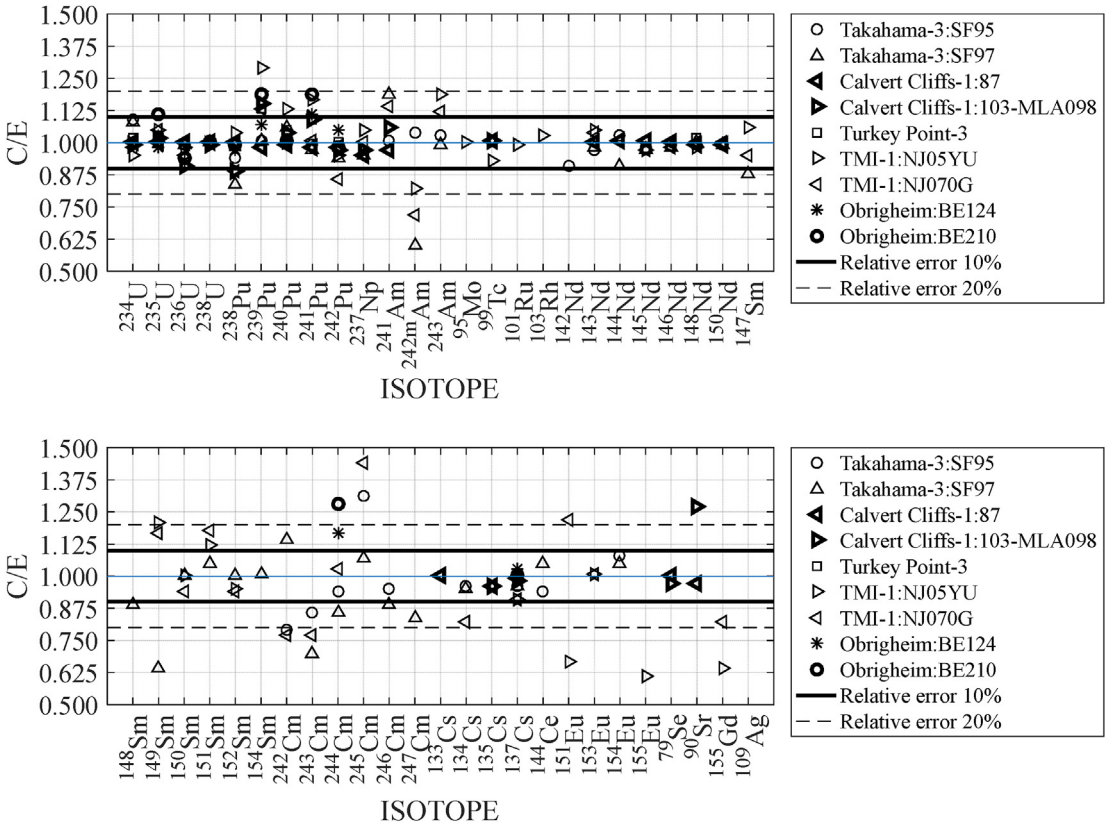

Fig. 13. Mean ratio of calculated-to-measured isotope inventories of five reactors.

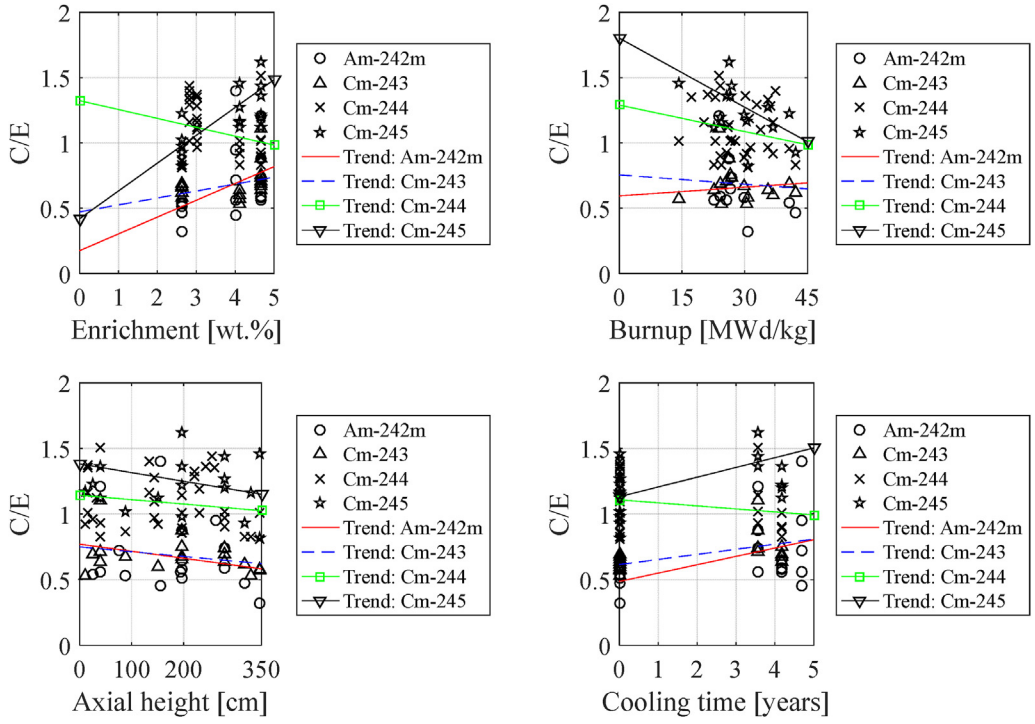

Fig. 14. Ratio of calculated-to-measured isotope inventories as a function of four parameters: enrichment, burnup, axial location of samples, and cooling time.

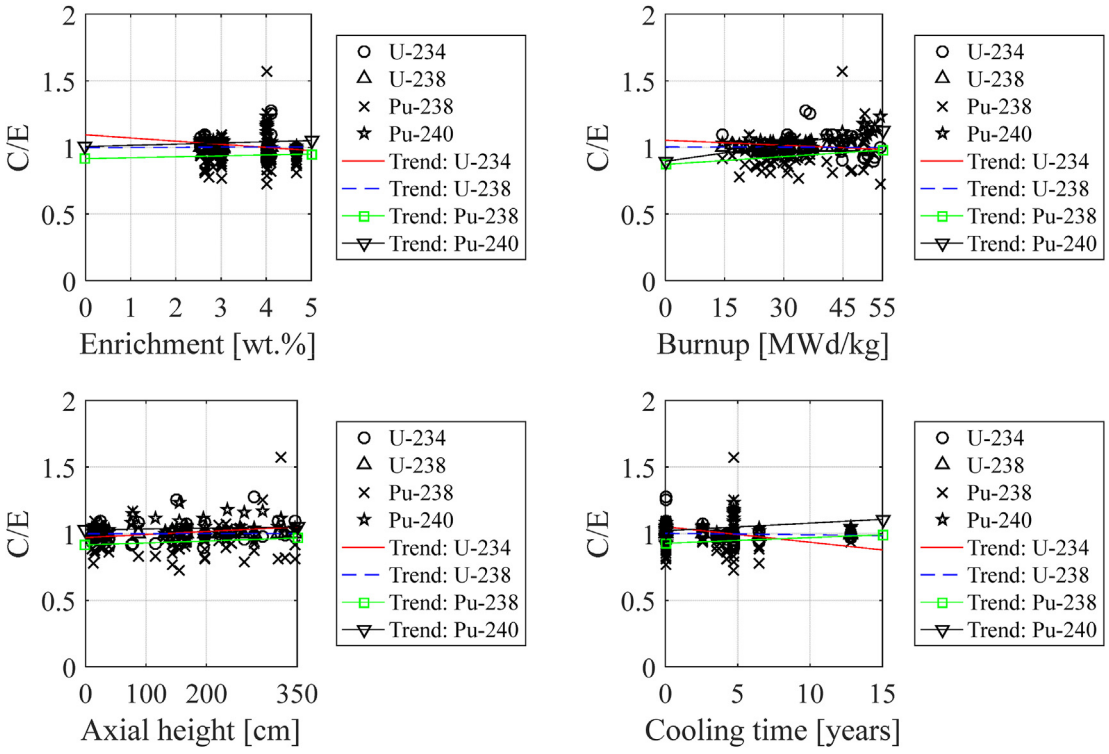

Fig. 15. Calculated-to-measured ratio of isotope inventories for four isotopes: ^{234}U, ^{238}U, ^{238}Pu, and ^{240}Pu.

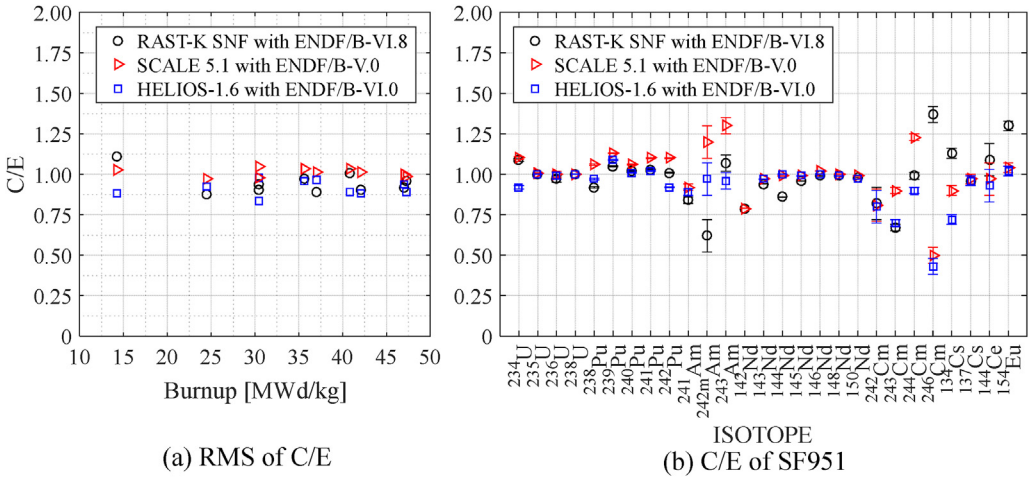

Fig. 16. Ratio of calculated-to-measured (C/E) isotope inventories of Takahama-3.

three codes was drawn with discharge burnup conditions of samples. The burnup range of the 58 samples is from 14.3 GWd/MTU to 55.7 GWd/MTU, and this burnup range covers the 11 high burnup samples (>45 GWd/MTU [27]). Takahama-3 and TMI-1 have two and nine high burnup samples, respectively. The relative difference is increasing as burnup proceeds as shown in subplot (a) of Figs. 16–21. The largest relative errors are seen at the highest burnup sample, D1A2 (55.7 GWd/MTU) discharged from TMI-1 as shown in Fig. 19. Although RAST-K SNF has largest C/E in the D1A2 sample, RAST-K SNF (RMS C/E of 1.31) has smaller RMS C/E than SCALE 5.1 (RMS C/E of 1.66). Fig. 20 presents the detail C/E of two highest burnup samples, B1B (discharged at 54.5 GWd/MTU) and D1A2. SCALE5.1 has larger relative errors compared with RAST-K SNF in those two samples as shown in subplot (a) of Fig. 20. RAST-K SNF has improved results in ^{243}Am, ^{151}Sm, and ^{152}Sm compared with SCALE 5.1. By contrast, SCALE 5.1 has slightly improved results in ^{241}Pu and ^{241}Am isotopes. RAST-K SNF has slightly overestimated ^{241}Pu and it could be responsible for the overestimated ^{241}Am content as beta decay.

As the burnup proceeds, fuel composition is changed by decay and fission reactions. The minor actinides ^{242m}Am and Cm have large absolute C/E as shown in Figs. 16–21. To assess the effect of mass ratio (*i.e.*, change of fuel composition) on C/E, the trend analysis of C/E is performed with mass ratio ($g/g_{\text{initial U}}$). Fig. 22 and Table A. 6 contain the trend analysis results of six isotopes: ^{242m}Am, ^{242}Cm, ^{243}Cm, ^{244}Cm, ^{245}Cm, and ^{246}Cm. The trend is calculated by least-square method [24] and linear-correlation coefficient is calculated following the reference [23]. Subplot (a) of Fig. 22

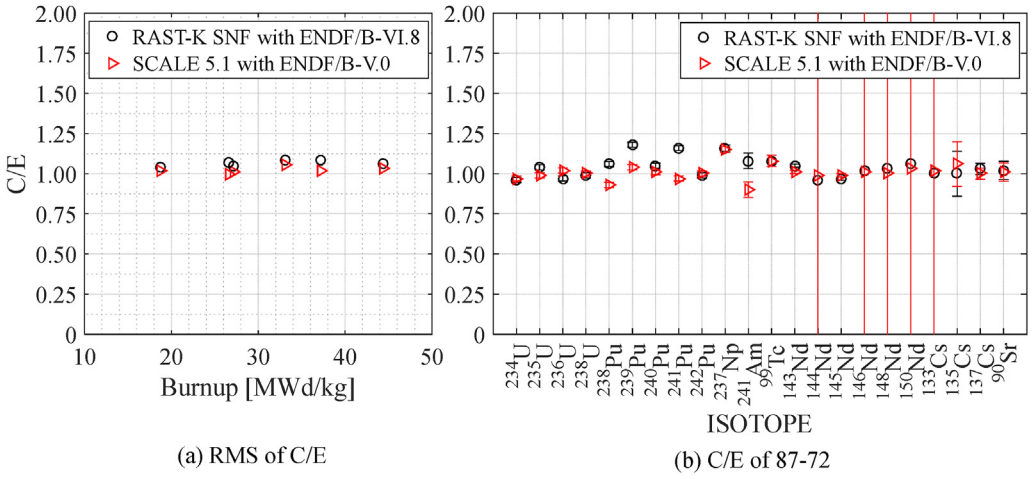

Fig. 17. Ratio of calculated-to-measured (C/E) isotope inventories of Calvert Cliffs-1.

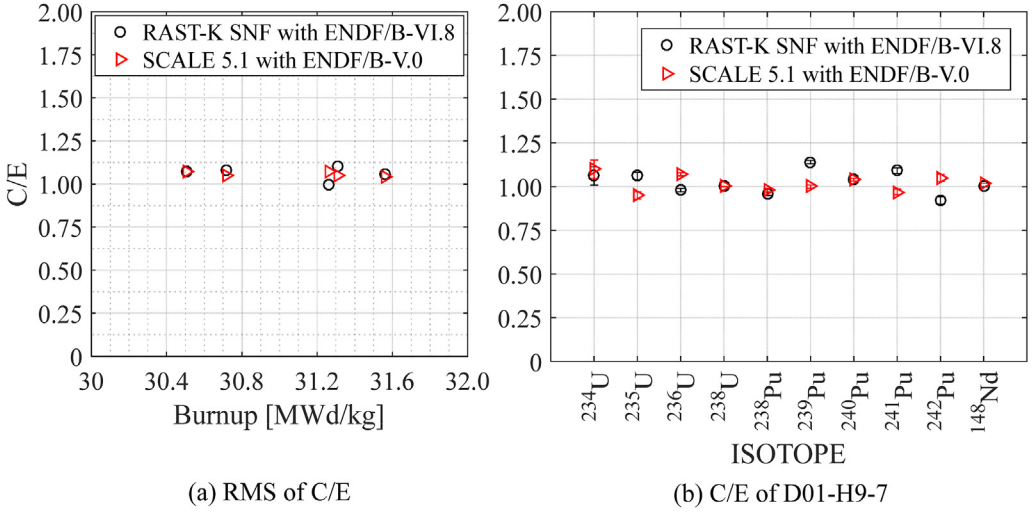

Fig. 18. Ratio of calculated-to-measured (C/E) isotope inventories of Turkey Point-3.

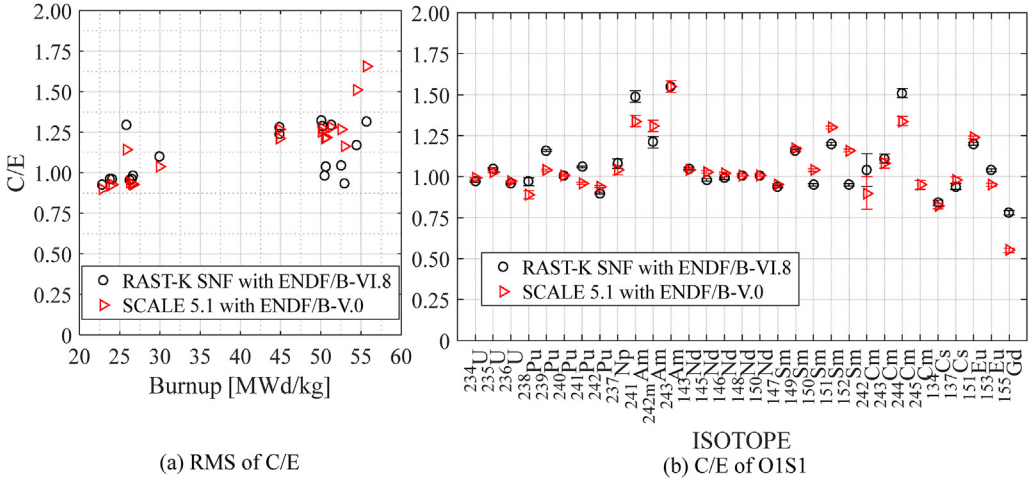

Fig. 19. Ratio of calculated-to-measured (C/E) isotope inventories of TMI-1.

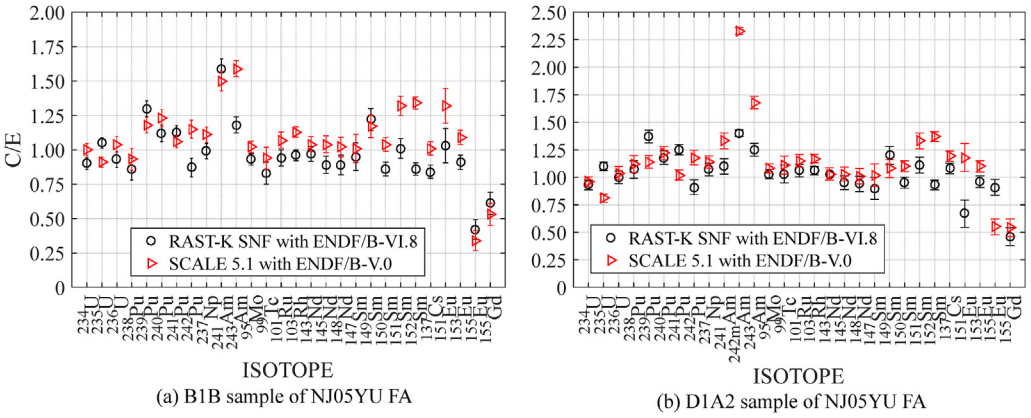

Fig. 20. Ratio of calculated-to-measured (C/E) isotope inventory for high burnup FA of TMI-1.

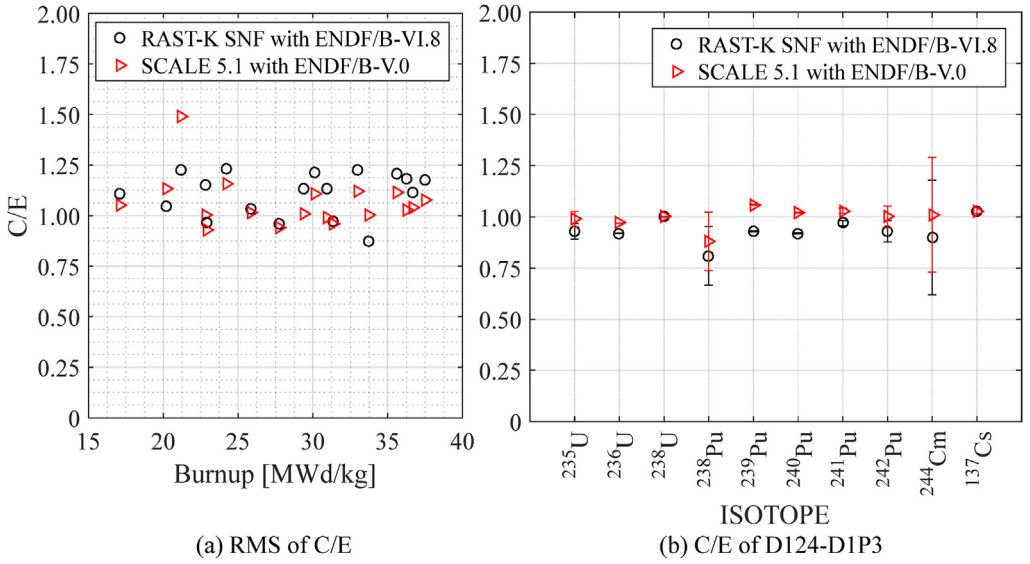

Fig. 21. Ratio of calculated-to-measured (C/E) isotope inventories of Obrigheim.

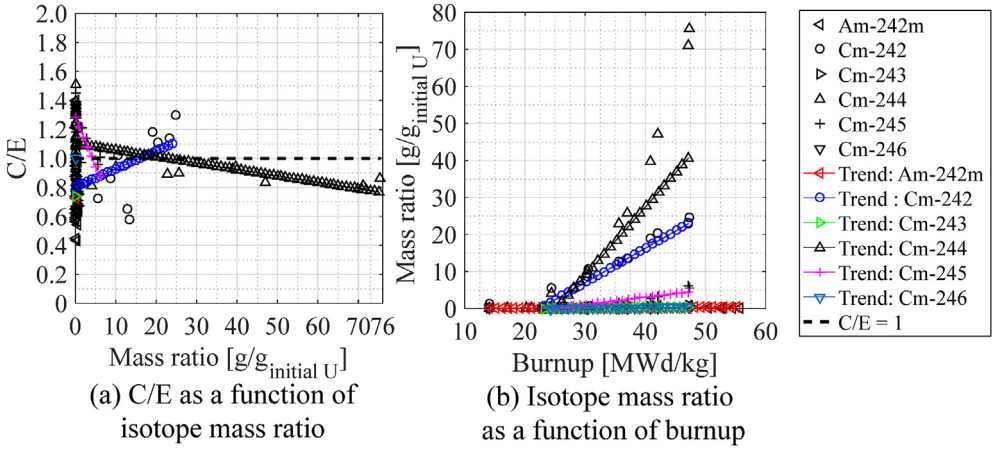

Fig. 22. Trend analysis of C/E and mass ratio with seven isotopes.

contains the ratio of calculated-to-measured (*i.e.*, C/E) as a function of isotope mass ratio and subplot (b) presents the isotope mass ratio as a function of discharge burnup. The trend is presented in the range of the benchmark sample mass ratios to assess the behavior of C/E in this interval. The isotopes: ^{242}Cm and ^{245}Cm are closer to 1 (*i.e.*, relative difference goes to zero) as the mass ratio

increases. Table A. 6 contains the details of linear correlation coefficient and trend. The C/E has strong correlation with mass ratio in ^{242}Cm, ^{244}Cm, and ^{245}Cm (*i.e.*, R^2 value is closer to 1 compared with other isotopes [23]). The subplot (b) of Fig. 22 and Table A. 6 show that ^{242}Cm ($R^2 = 0.8441$), ^{243}Cm ($R^2 = 0.8712$), and ^{245}Cm ($R^2 = 0.8092$) have stronger correlation between burnup and isotope mass ratio compared with ^{246}Cm ($R^2 = 0.6869$), ^{244}Cm ($R^2 = 0.5373$), ^{242m}Am ($R^2 = 0.0235$). To assess the dominant effect on C/E, comparison of linear correlation coefficient is performed. ^{246}Cm has the strongest correlation with mass ratio, compared with burnup. For this nuclide, the linear correlation coefficient with discharge burnup is farther from 1 than the mass ratio condition. By contrast, ^{245}Cm has the strongest relationship with discharge burnup condition compared with mass ratio.

These comparisons show that RAST-K SNF can generate reasonable calculation results with accuracy comparable to SCALE 5.1 and HELIOS-1.6.

4. Conclusion

An SNF analysis method for the prediction of the isotope inventory was validated in this study. RAST-K SNF was developed using the STREAM/RAST-K two-step code system to improve the speed of the calculation. A Lagrange interpolation and the power history correction factors were used to replace the depletion calculation during the SNF analysis. To assess the accuracy of developed code system, validation study was performed with a total of 58 benchmark assays. The targeted SNF applications are engineering design studies of reactor components (shielding and maintenance schedules), burnup credit criticality safety analysis, and management of radioactive wastes (evaluation of expected masses and costs of waste disposal). Selected benchmark samples cover UO_2 enrichment range of 2.556–4.657 wt%, a discharge burnup from 14.3 to 55.7 GWd/MTU, and a cooling times from 2.54 to 12.76 years. ENDF/B-VII.0 library and pin model are used for the calculations.

The validation study presents the average relative difference (C/E−1) within ±4% for the actinides ^{234}U, ^{235}U, ^{236}U, ^{238}U, ^{238}Pu, ^{240}Pu, ^{242}Pu, and ^{237}Np and fission products ^{95}Mo, ^{101}Ru, ^{103}Ru, ^{143}Nd, ^{144}Nd, ^{145}Nd, ^{146}Nd, ^{148}Nd, ^{150}Nd, ^{147}Sm, ^{150}Sm, ^{152}Sm, ^{154}Sm, ^{133}Cs, ^{135}Cs, ^{137}Cs, ^{144}Ce, ^{153}Eu, and ^{90}Sr. In addition, the average relative differences are within ±12% for ^{241}Am, ^{242}Cm, ^{244}Cm, and ^{246}Cm isotopes which are of importance in shielding analysis. In addition, a verification study was performed in this study with HELIOS-1.6 and SCALE5.1. A total of 10 samples of Takahama-3 are used for comparison with HELIOS-1.6 and 58 samples are used for comparison with SCALE 5.1. This verification study presents that the developed code system can provide reasonable results with accuracy comparable with those code systems.

We plan to predict the isotope inventory of SNF assemblies discharged from full cycles of PWRs in South Korea and suggest an optimum pattern of spent fuel storage casks for safety and greater financial gain.

Declaration of competing interest

The authors declare that they have no known competing financial interests or personal relationships that could have appeared to influence the work reported in this paper.

Acknowledgments

This work was supported by the National Research Foundation of Korea (NRF) grant funded by the Korea government (MSIT). (No. NRF-2019M2D2A1A03058371).

Appendix

Table A. 1 contains the mean ratio of calculated-to-measured isotope inventories. Tables A. 2 and A. 3 describe the verification results with STREAM-SNF. Tables A. 2 and A. 3 contain the comparison data of actinides and fission products, respectively. Tables A. 4 and A. 5 contain the detail error trend analysis results of Am, Cm, U and P isotopes. Table A. 6 presents the trend analysis results of Am and Cm with mass ratio and discharge burnup.

Fig. A. 1 through Fig. A. 11 show the relative errors (C/E−1) of the nuclides with measurement uncertainties [14], and the graphs contain the results of ^{234}U, ^{235}U, ^{236}U, ^{238}U, ^{238}Pu, ^{239}Pu, ^{240}Pu, ^{241}Pu, ^{242}Pu, ^{237}Np, ^{241}Am, ^{242m}Am, ^{243}Am, ^{95}Mo, ^{99}Tc, ^{101}Ru, ^{103}Rh, ^{143}Nd, ^{145}Nd, ^{147}Sm, ^{149}Sm, ^{150}Sm, ^{151}Sm, ^{152}Sm, ^{151}Eu, and ^{153}Eu.

Table A. 1
Mean ratios of calculated-to-measured ($\overline{C/E}$) isotope inventory of Takahama-3 samples as compared with the measurements

ISOTOPE	$1\sigma_M$[a] [%]	SF95				SF97			
		STREAM-SNF		RAST-K SNF		STREAM-SNF		RAST-K SNF	
		$\overline{C/E}$[b]	$1\sigma_C$[c]	$\overline{C/E}$	$1\sigma_C$	$\overline{C/E}$	$1\sigma_C$	$\overline{C/E}$	$1\sigma_C$
^{234}U	1	1.12	0.14	1.09	0.10	1.07	0.02	1.08	0.01
^{235}U	0.1	1.00	0.01	1.01	0.01	1.00	0.03	1.02	0.05
^{236}U	2	0.98	0.01	0.99	0.03	0.98	0.00	0.99	0.01
^{238}U	0.1	1.00	0.00	1.00	0.00	1.00	0.00	1.00	0.00
^{237}Np	10					0.96	0.01	0.95	0.01
^{238}Pu	0.5	0.88	0.05	0.94	0.10	0.85	0.03	0.84	0.04
^{239}Pu	0.3	1.00	0.03	1.01	0.02	1.01	0.03	1.01	0.04
^{240}Pu	0.3	1.01	0.02	1.01	0.03	1.06	0.02	1.06	0.02
^{241}Pu	0.3	0.95	0.03	0.99	0.04	0.97	0.04	0.97	0.04
^{242}Pu	0.3	0.94	0.02	0.97	0.05	0.95	0.00	0.94	0.02
^{241}Am	2	1.02	0.13	1.01	0.15	1.19	0.08	1.19	0.10
^{242m}Am	10	0.55	0.04	1.04	0.51	0.59	0.04	0.60	0.09
^{243}Am	5	1.01	0.05	1.03	0.04	1.01	0.03	0.99	0.04
^{242}Cm	10	0.70	0.10	0.79	0.23	1.15	0.10	1.14	0.10
^{243}Cm	2	0.64	0.05	0.86	0.41	0.72	0.04	0.70	0.05
^{244}Cm	2	0.88	0.09	0.94	0.08	0.89	0.05	0.86	0.06
^{245}Cm	2	0.98	0.11	1.31	0.47	0.97	0.10	1.07	0.13
^{246}Cm	5	0.88	0.39	0.95	0.28	0.87	0.05	0.89	0.08
^{247}Cm						0.79	0.06	0.84	0.08
^{142}Nd		0.83	0.05	0.91	0.13				
^{143}Nd	0.1	0.95	0.00	0.97	0.04	0.97	0.01	0.98	0.01
^{144}Nd	0.1	0.96	0.02	1.03	0.12	0.95	0.02	0.91	0.03
^{145}Nd	0.1	0.97	0.00	0.98	0.03	0.98	0.00	0.97	0.01
^{146}Nd	0.1	0.99	0.00	0.99	0.00	0.99	0.00	0.98	0.01
^{148}Nd	0.1	0.99	0.00	0.99	0.01	0.99	0.00	1.00	0.01
^{150}Nd	0.1	0.97	0.01	0.99	0.02	1.00	0.00	0.99	0.01
^{137}Cs	3	0.96	0.01	0.96	0.04	0.96	0.00	0.96	0.01
^{134}Cs	3	0.92	0.02	0.96	0.13	0.92	0.04	0.95	0.02
^{154}Eu	3	0.99	0.03	1.08	0.13	1.01	0.04	1.05	0.04
^{144}Ce	10	0.97	0.03	0.94	0.13	0.98	0.06	1.05	0.09
^{147}Sm	0.1					1.01	0.01	0.88	0.25
^{148}Sm	0.1					0.90	0.01	0.89	0.02
^{149}Sm	0.1					0.63	0.02	0.64	0.03
^{150}Sm	0.1					1.00	0.01	1.00	0.02
^{151}Sm	0.1					0.97	0.05	1.05	0.06
^{152}Sm	0.1					1.02	0.02	1.00	0.02
^{154}Sm	0.1					1.02	0.01	1.01	0.01

a. σ_M is the standard deviation of the measurements [14].
b. $\overline{C/E}$ is the mean of the ratio of calculated-to-experimental isotope inventories.
c. σ_C is the standard deviation of the calculated isotope inventory, $\sigma_C = \sqrt{\frac{\sum_{i=1}^{N}(x_i - \overline{x})^2}{N}}$, where x is the value of C/E, $\overline{x}$ is the mean value of C/E, and N is the total number of calculated results.

Table A. 2
Ratio of calculated-to-measured isotope inventories compared with STREAM-SNF for actinides

Isotope	Number of samples	RAST-K SNF		STREAM-SNF		Relative difference	
		$\overline{C/E}^b$	$1\sigma_C{}^c$	$\overline{C/E}$	$1\sigma_C$	$Diff_{avg}{}^d$ [%]	$1\sigma_{avg}{}^e$ [%]
^{234}U	40	1.01	0.07	1.01	0.08	0	4
^{235}U	58	1.03	0.06	1.03	0.06	1	2
^{236}U	58	0.96	0.04	0.97	0.04	−1	2
^{238}U	39	1.00	0.01	1.00	0.01	0	1
^{238}Pu	58	0.96	0.13	0.97	0.14	−1	4
^{239}Pu	58	1.13	0.12	1.14	0.12	−1	5
^{240}Pu	58	1.03	0.06	1.03	0.07	0	3
^{241}Pu	58	1.09	0.10	1.10	0.10	−1	4
^{242}Pu	58	0.97	0.08	0.98	0.09	−1	3
^{237}Np	30	1.00	0.06	1.03	0.07	−2	6
^{241}Am	34	1.09	0.17	1.11	0.17	−2	10
^{242m}Am	23	0.78	0.34	0.71	0.26	10	33
^{243}Am	29	1.11	0.16	1.12	0.15	−1	3
^{242}Cm	18	0.88	0.23	0.87	0.22	1	9
^{243}Cm	18	0.78	0.23	0.74	0.11	6	34
^{244}Cm	35	1.08	0.21	1.10	0.20	−2	3
^{245}Cm	18	1.30	0.36	1.21	0.31	9	25
^{246}Cm	10	0.92	0.20	0.92	0.25	8	42
^{247}Cm	5	0.84	0.08	0.79	0.07	6	8

For *b* and *c*, see the footnotes of Table A. 1.

d is mean relative difference [%], $Diff_{avg} = \left(\frac{1}{n}\sum_{i=1}^{n}\left(\frac{C_{RAST-K\ SNF}}{C_{STREAM-SNF}} - 1\right)\right)*100$ [%], where *n* is the number of samples; and.

e is the standard deviation of the relative difference [%], $\sigma_{avg} = \sqrt{\frac{\sum_{i=1}^{n}(x_i - \bar{x})^2}{n}}$, where x is the value of $C_{RAST\text{-}K\ SNF}/C_{STREAM\text{-}SNF}$, $\bar{x}$ is the mean value of $C_{RAST\text{-}K\ SNF}/C_{STREAM\text{-}SNF}$, and *N* is the number of samples.

Table A. 3
Ratio of calculated-to-measured isotope inventories compared with STREAM-SNF for fission products

Isotope	Number of samples	RAST-K SNF		STREAM-SNF		Relative difference	
		$\overline{C/E}^b$	$1\sigma_C{}^c$	$\overline{C/E}$	$1\sigma_C$	$Diff_{avg}{}^d$ [%]	$1\sigma_{avg}{}^e$ [%]
^{95}Mo	11	1.00	0.06	0.97	0.06	4	3
^{99}Tc	17	0.95	0.11	0.96	0.12	−1	3
^{101}Ru	11	0.99	0.08	0.99	0.07	0	3
^{103}Rh	11	1.03	0.08	1.07	0.07	−4	2
^{142}Nd	5	0.91	0.13	0.84	0.06	7	10
^{143}Nd	32	1.02	0.06	1.02	0.06	0	3
^{144}Nd	13	0.98	0.10	0.96	0.02	2	9
^{145}Nd	32	0.98	0.04	0.97	0.04	0	3
^{146}Nd	21	0.99	0.01	0.99	0.01	0	1
^{148}Nd	37	0.99	0.04	0.99	0.04	0	2
^{150}Nd	21	0.99	0.02	1.00	0.02	−1	3
^{147}Sm	24	0.99	0.15	1.01	0.08	−2	13
^{148}Sm	5	0.89	0.02	0.90	0.01	−1	1
^{149}Sm	24	1.08	0.25	1.09	0.26	−1	2
^{150}Sm	24	0.98	0.08	1.02	0.11	−3	4
^{151}Sm	24	1.12	0.09	1.15	0.14	−2	7
^{152}Sm	24	0.96	0.05	0.97	0.06	−1	2
^{154}Sm	5	1.01	0.01	1.02	0.01	0	2
^{133}Cs	3	1.00	0.01	0.99	0.01	1	2
^{134}Cs	18	0.89	0.10	0.88	0.07	1	7
^{135}Cs	6	0.96	0.05	1.01	0.10	−4	9
^{137}Cs	50	0.96	0.06	0.97	0.05	−1	3
^{144}Ce	10	0.99	0.12	0.97	0.05	2	15
^{151}Eu	19	0.90	0.32	0.93	0.31	−2	15
^{153}Eu	19	1.01	0.06	1.01	0.06	0	2
^{154}Eu	10	1.07	0.09	1.03	0.05	4	6
^{155}Eu	11	0.61	0.12	0.64	0.10	−5	11
^{90}Sr	6	0.98	0.02	0.99	0.01	0	2
^{79}Se	6	1.31	0.06	1.30	0.06	1	0
^{155}Gd	19	0.72	0.13	0.76	0.13	−5	12
^{109}Ag	11	1.54	0.38	1.57	0.38	−2	3

For *b*, *c*, *d*, and *e*, see the footnotes of Table A. 2.

Table A. 4
Error trend analysis of Am and Cm

Isotope	Parameter	R^2 [a]	Trend [b]
^{242m}Am	Enrichment [wt.%]	0.1647	y [c] $= 0.1287\ x$ [d] $+ 0.1752$
	Burnup [MWd/kg]	0.0104	$y = 0.0022\ x + 0.5947$
	Axial height [cm]	0.0396	$y = -0.0005\ x + 0.7707$
	Cooling time [years]	0.2095	$y = 0.0636\ x + 0.4866$
^{243}Cm	Enrichment [wt.%]	0.1154	$y = 0.0532\ x + 0.4724$
	Burnup [MWd/kg]	0.0246	$y = -0.0024\ x + 0.7555$
	Axial height [cm]	0.1051	$y = -0.0004\ x + 0.7504$
	Cooling time [years]	0.3221	$y = 0.0388\ x + 0.6154$
^{244}Cm	Enrichment [wt.%]	0.0700	$y = -0.0682\ x + 1.3240$
	Burnup [MWd/kg]	0.0652	$y = -0.0068\ x + 1.2900$
	Axial height [cm]	0.0315	$y = -0.0003\ x + 1.1440$
	Cooling time [years]	0.0343	$y = -0.0231\ x + 1.1090$
^{245}Cm	Enrichment [wt.%]	0.3665	$y = 0.2130\ x + 0.4199$
	Burnup [MWd/kg]	0.2688	$y = -0.0176\ x + 1.8030$
	Axial height [cm]	0.0683	$y = -0.0007\ x + 1.3830$
	Cooling time [years]	0.2345	$y = 0.0743\ x + 1.1320$

a is Linear-correlation coefficient. The closer the coefficient approaches a value of 1, the better the fit is to the linear trend [23]; *b* is trend calculated using least-square method [24]; *c* indicates the ratio of calculated-to-measured (C/E) isotope inventories; *d* is a parameter.

Table A. 5
Error trend analysis with U and Pu

Isotope	Parameter	R^2 [a]	Trend [b]
^{234}U	Enrichment [wt.%]	0.0591	y [c] $= -0.0239\ x$ [d] $+ 1.0950$
	Burnup [MWd/kg]	0.0340	$y = -0.0013\ x + 1.0550$
	Axial height [cm]	0.0906	$y = 0.0002\ x + 0.9710$
	Cooling time [years]	0.2325	$y = -0.0116\ x + 1.0520$
^{238}U	Enrichment [wt.%]	0.0049	$y = 0.0013\ x + 0.9973$
	Burnup [MWd/kg]	0.0064	$y = -0.0001\ x + 1.0040$
	Axial height [cm]	0.0037	$y \cong 1$
	Cooling time [years]	0.2179	$y = -0.0012\ x + 1.0030$
^{238}Pu	Enrichment [wt.%]	0.0016	$y = 0.0069\ x + 0.9153$
	Burnup [MWd/kg]	0.0260	$y = 0.0020\ x + 0.8723$
	Axial height [cm]	0.0135	$y = 0.0001\ x + 0.9160$
	Cooling time [years]	0.0116	$y = 0.0042\ x + 0.9276$
^{240}Pu	Enrichment [wt.%]	0.0127	$y = 0.0091\ x + 1.0070$
	Burnup [MWd/kg]	0.5445	$y = 0.0042\ x + 0.8965$
	Axial height [cm]	0.0112	$y = 0.0001\ x + 1.0290$
	Cooling time [years]	0.0964	$y = 0.0057\ x + 1.0230$

a, *b*, *c* and *d* see the footnotes of Table A. 4.

Table A. 6
Trend analysis of Am and Cm with mass ratio and discharge burnup

Figure	Isotope	R^2 [a]	Trend [b]
Subplot (a) of Fig. 22	^{242m}Am	3.3290e-06	y [c] $= 0.0015\ x$ [d] $+ 0.7244$
	^{242}Cm	0.3316	$y = 0.0124\ x + 0.8032$
	^{243}Cm	0.0233	$y = -0.0771\ x + 0.7410$
	^{244}Cm	0.1880	$y = -0.0044\ x + 1.0990$
	^{245}Cm	0.1295	$y = -0.0684\ x + 1.2850$
	^{246}Cm	0.1595	$y = -0.4540\ x + 1.0000$
Subplot (b) of Fig. 22	^{242m}Am	0.0235	$y = 0.0039\ x + 0.0980$
	^{242}Cm	0.8441	$y = 0.9283\ x - 20.8600$
	^{243}Cm	0.8712	$y = 0.0231\ x - 0.5408$
	^{244}Cm	0.5373	$y = 1.8510\ x - 46.6500$
	^{245}Cm	0.8092	$y = 0.1948\ x - 4.7790$
	^{246}Cm	0.6869	$y = 0.0179\ x - 0.4320$

a, *b*, *c* and *d* see the footnotes of Table A. 4.

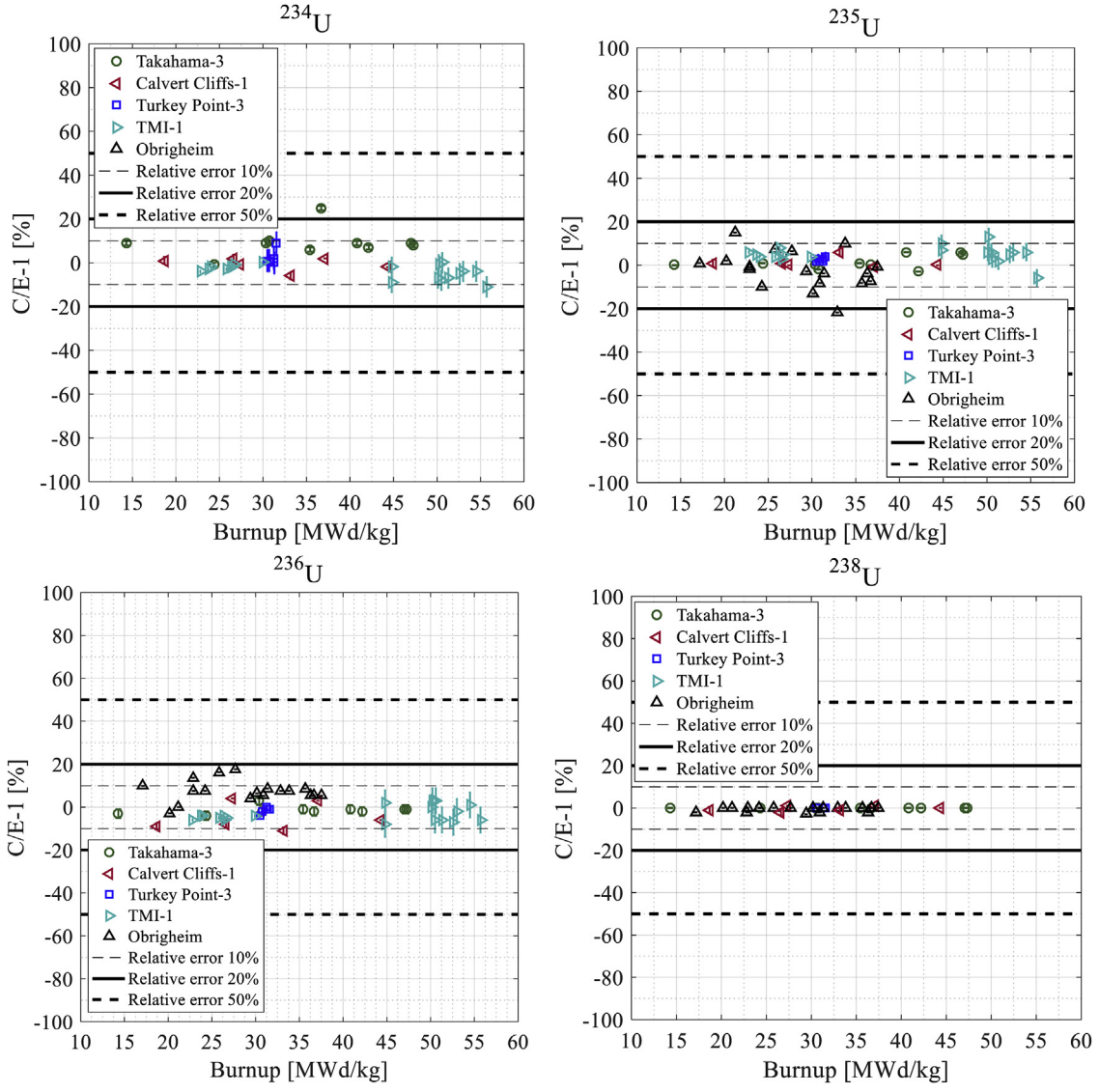

Fig. A. 1. Relative differences in concentration of U isotopes versus sample burnup.

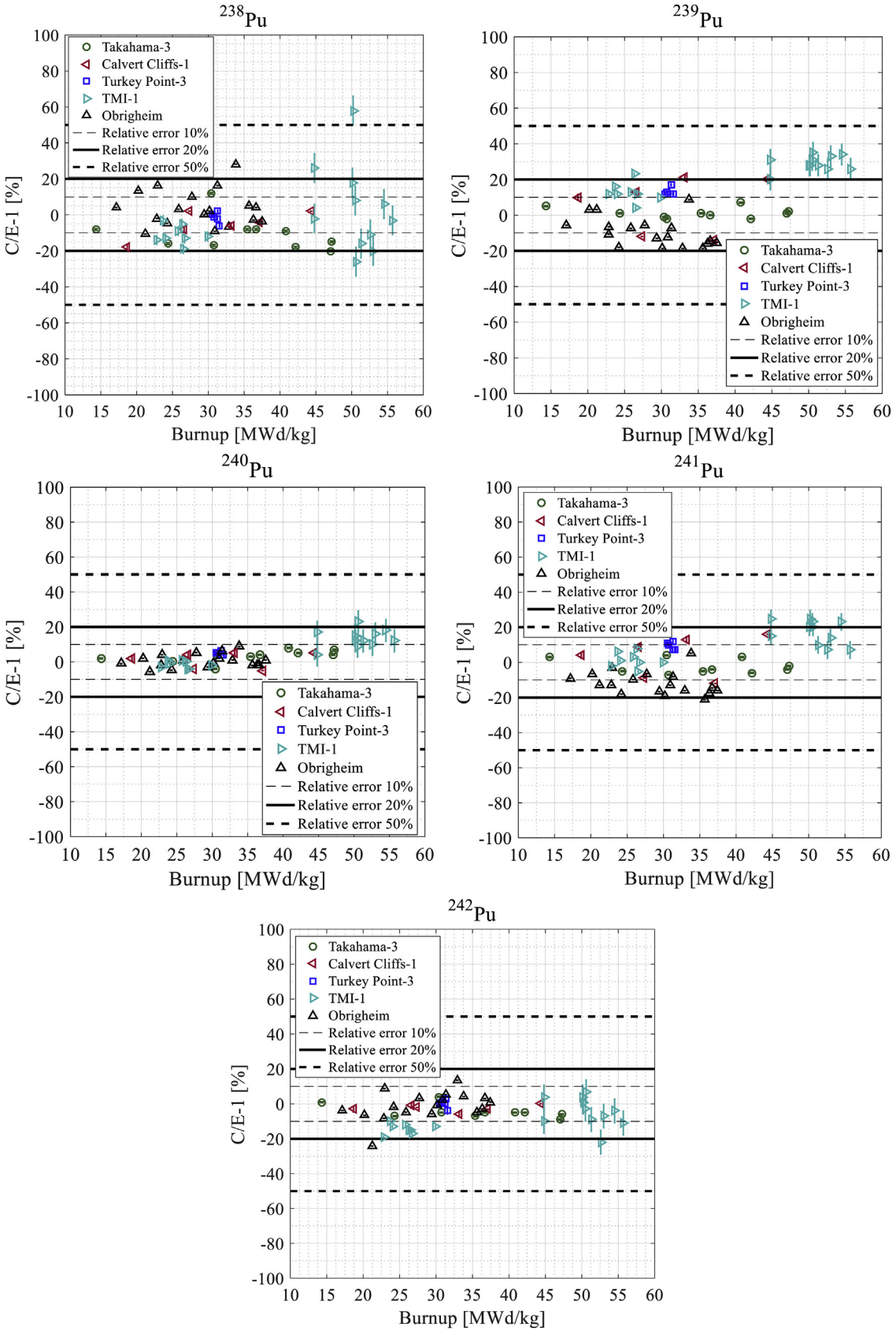

Fig. A. 2. Relative differences in concentration of Pu isotopes versus sample burnup.

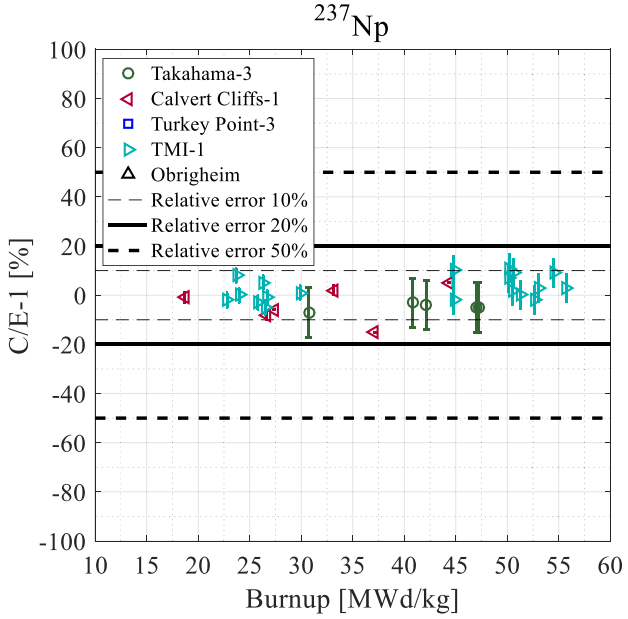

Fig. A. 3. Relative differences in ^{237}Np concentration versus sample burnup.

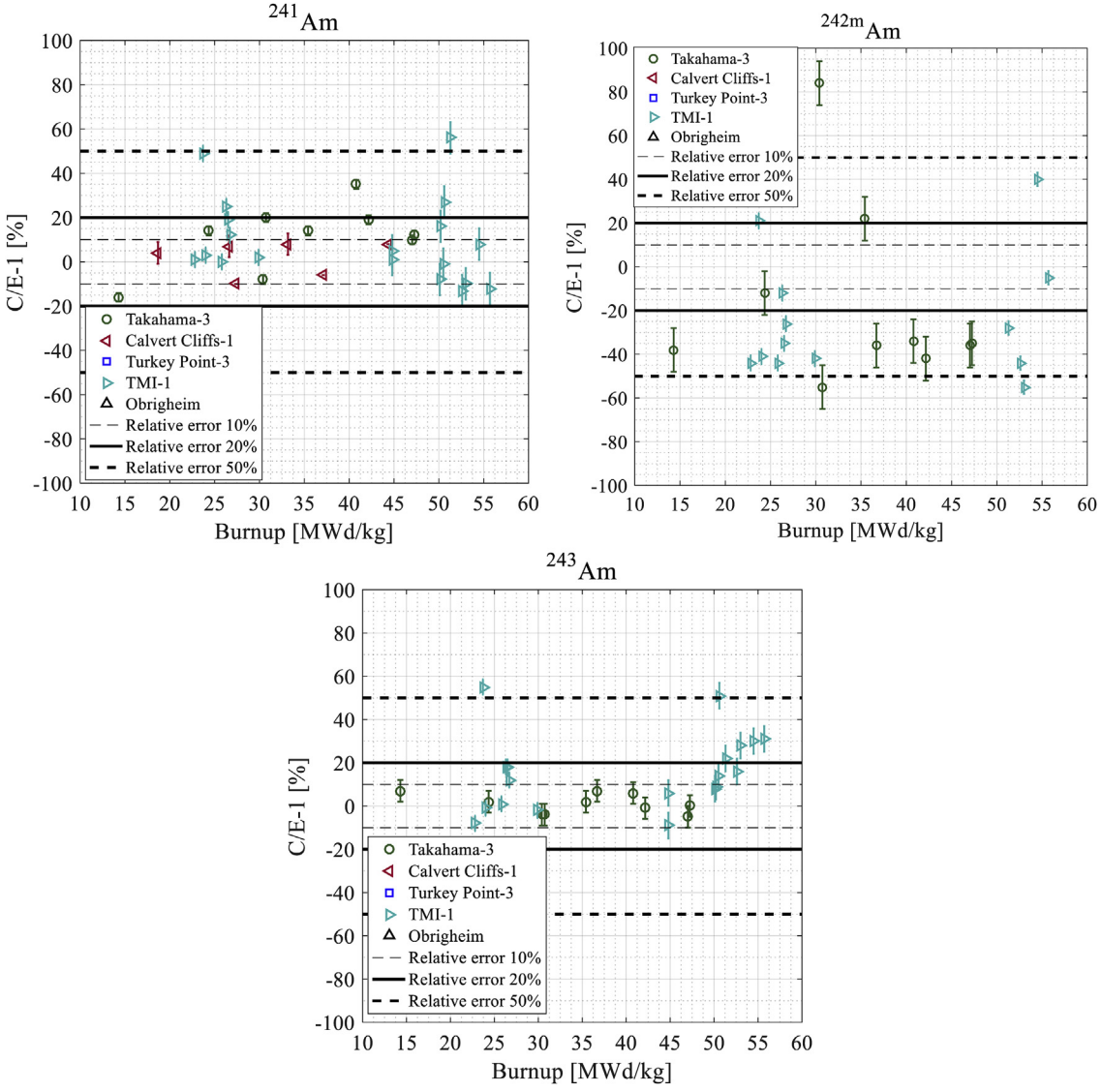

Fig. A. 4. Relative differences in concentration of Am isotopes versus sample burnup.

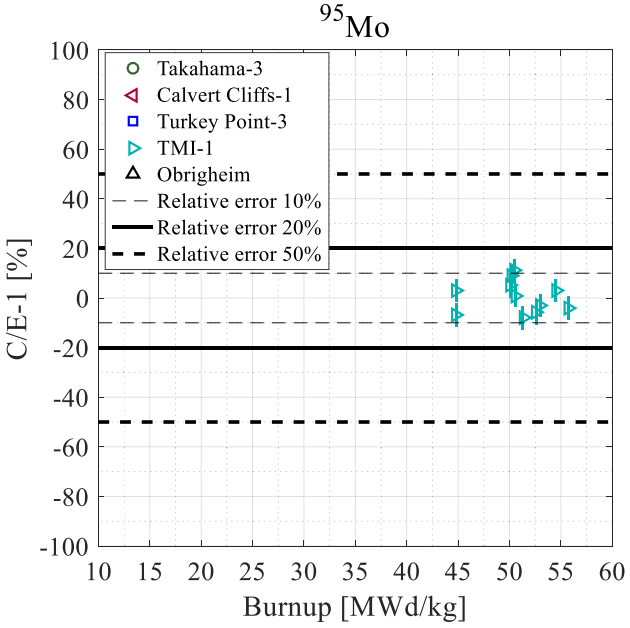

Fig. A. 5. Relative differences in ^{95}Mo concentration versus sample burnup.

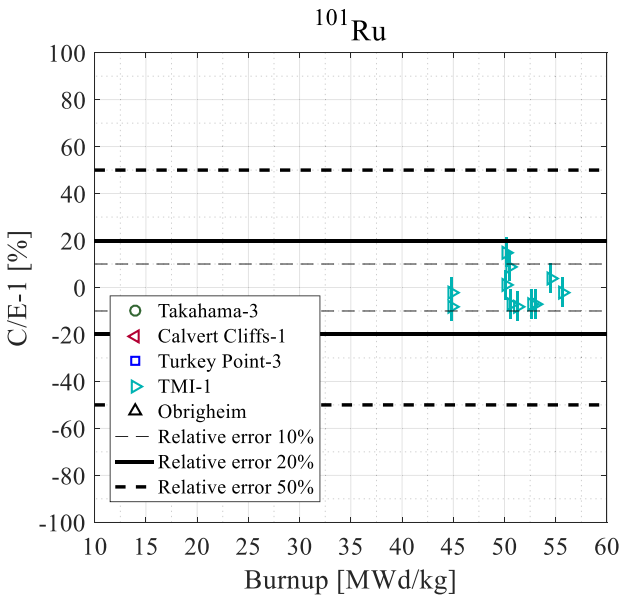

Fig. A. 7. Relative differences in ^{101}Ru concentration versus sample burnup.

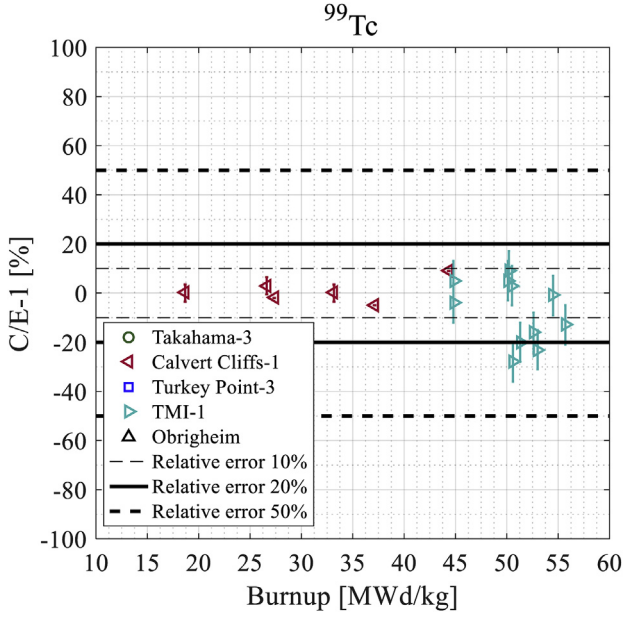

Fig. A. 6. Relative differences in ^{99}Tc concentration versus sample burnup.

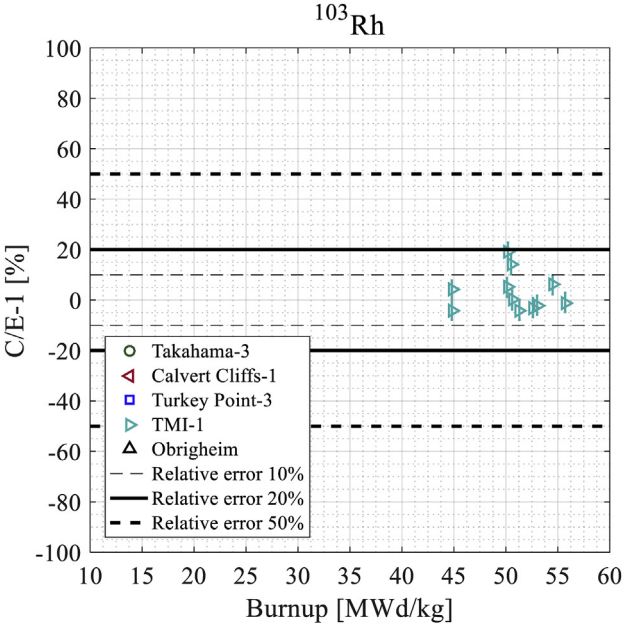

Fig. A. 8. Relative differences in ^{103}Rh concentration versus sample burnup.

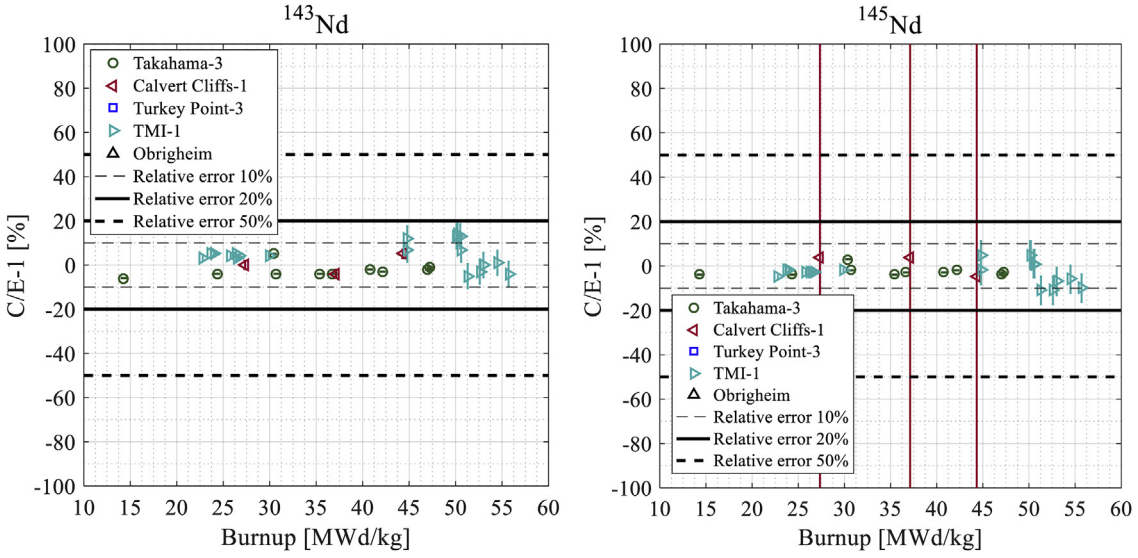

Fig. A. 9. Relative differences in concentration of Nd isotopes versus sample burnup.

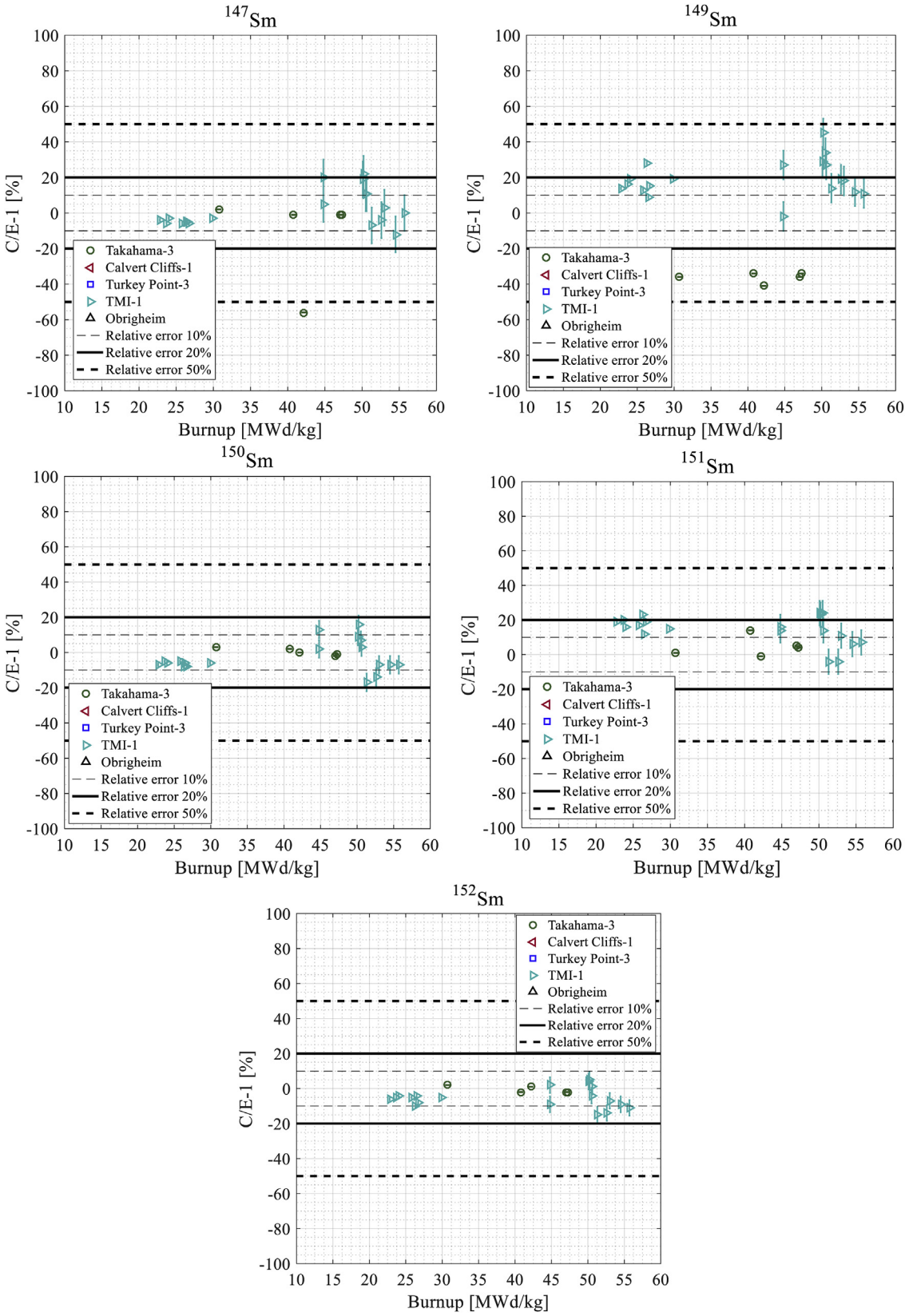

Fig. A. 10. Relative differences in concentration of Sm isotopes versus sample burnup.

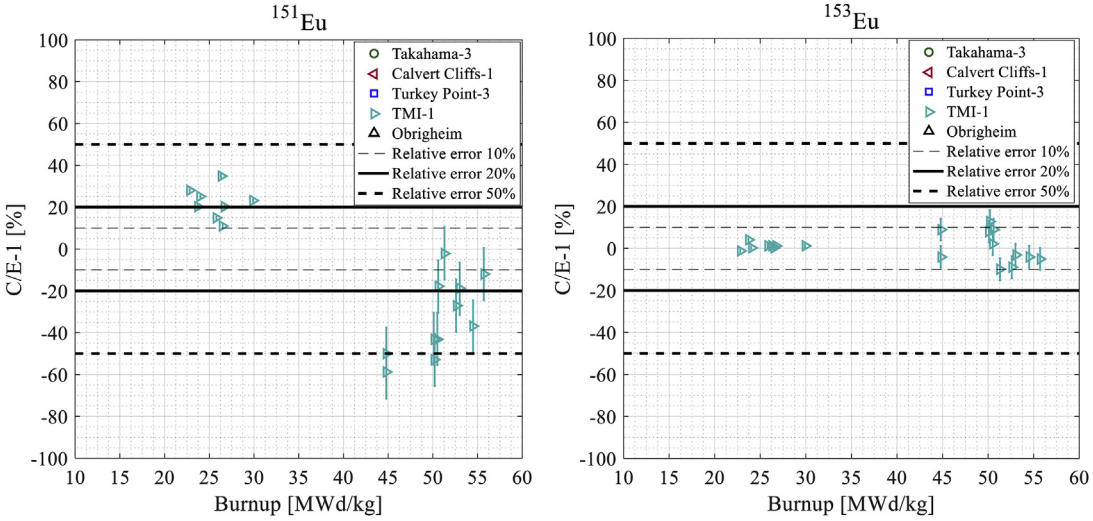

Fig. A. 11. Relative differences in concentration of Eu isotopes versus sample burnup.

Appendix A. Supplementary data

Supplementary data to this article can be found online at https://doi.org/10.1016/j.net.2021.01.009.

References

[1] B. Ebiwonjumi, S. Choi, M. Lemaire, D. Lee, H.C. Shin, H.S. Lee, Validation of lattice physics code STREAM for predicting pressurized water reactor spent nuclear fuel isotopic inventory, Ann. Nucl. Energy 120 (2018) 431–449, https://doi.org/10.1016/j.anucene.2018.06.002.

[2] A. Mohammadi, M. Hassanzadeh, M. Gharib, Shielding calculation and criticality safety analysis of spent fuel transportation cask in research reactors, Appl. Radiat. Isot. 108 (2016) 129–132.

[3] N. Mai, P.Z.M. Lemaire, B. Ebiwonjumi, W. Kim, H. Lee, D. Lee, Extension of Monte Carlo code MCS to spent fuel cask shielding analysis, Int. J. Energy Res. 44 (2020) 8089–8102, https://doi.org/10.1002/er.5023.

[4] J. Jang, W. Kim, S. Jeong, E. Jeong, J. Park, M. Lemaire, H. Lee, Y. Jo, P. Zhang, D. Lee, Validation of UNIST Monte Carlo code MCS for criticality safety analysis of PWR spent fuel pool and storage cask, Ann. Nucl. Energy 114 (2018) 495–509.

[5] NUREG/CR-6747, Computational Benchmark for Estimation of Reactivity Margin from Fission Products and Minor Actinides in PWR Burnup Credit, ORNL, 2001. ORNL/TM-2000/306.

[6] J.-Ch. Sublet, J.W. Eastwood, J.G. Morgan, M.R. Gilbert, M. Fleming, W. Arter, FISPACT-II: an advanced simulation system for activation, in: Transmutation and Material Modelling, Nuclear Data Sheets 139, 2017, pp. 77–173, https://doi.org/10.1016/j.nds.2017.01.002.

[7] Status of spent fuel storage for the first quarter of 2019 [Online] (available from: http://www.khnp.co.kr/board/BRD_000179/boardView.do?pageIndex=1&boardSeq=70138&mnCd=FN051304&schPageUnit=10&searchCondition=0&searchKeyword=, 2019e. Accessed on April 2019.

[8] S. Choi, C. Lee, D. Lee, Resonance treatment using pin-based pointwise energy slowing-down method, J. Comput. Phys. 330 (2017) 134–155.

[9] S. Choi, D. Lee, Three-dimensional method of characteristics/diamond-difference transport analysis method in STREAM for whole-core neutron transport calculation, Comput. Phys. Commun. (2020), https://doi.org/10.1016/j.cpc.2020.107332.

[10] M.B. Chadwick, ENDF/B-VII.0: next generation evaluated nuclear data library for nuclear science and technology, Nucl. Data Sheets 107 (12) (2006) 2931–3060, https://doi.org/10.1016/j.nds.2006.11.001.

[11] J. Jang, B. Ebiwonjumi, W. Kim, J. Park, D. Lee, Verification and Validation of Back-End Cycle Source Term Calculation of the Nodal Code RAST-K, PHYSOR 2020: Transition to a Scalable Nuclear Future Cambridge, United Kingdom, March 29–April 2, 2020.

[12] J. Jang, B. Ebiwonjumi, W. Kim, J. Park, J. Choe, D. Lee., Validation of spent nuclear fuel decay heat calculation by a two-step method, Nucl. Eng. Tech, accepted to publish, https://doi.org/10.1016/j.net.2020.06.028.

[13] B. Ebiwonjumi, S. Choi, M. Lemaire, D. Lee, H.C. Shin, H.S. Lee, Verification and validation of radiation source term capabilities in STREAM, Ann. Nucl. Energy 124 (2019) 80–87, https://doi.org/10.1016/j.anucene.2018.09.034.

[14] G. Radulescu, I.C. Gauld, G. Ilas, SCALE 5.1 Predictions of PWR Spent Nuclear Fuel Isotopic Compositions, March 2010. ORNL/TM-2010/44.

[15] J. Choe, S. Choi, P. Zhang, J. Park, W. Kim, H.C. Shin, H.S. Lee, J. Jung, D. Lee, Verification and validation of STREAM/RAST-K for PWR analysis, Nucl. Eng. Tech. 51 (2) (2019) 356–368.

[16] J. Park, J. Choe, H. Kim, S. Choi, A. Cherezov, J. Jang, D. Yun, N.N.T. Mai, V. Dos, D. Lee, H.C. Shin, H.S. Lee, Development status of nodal diffusion code RAST-K v2.2, in: KNS Spring Meeting Jeju, May 22–24, 2019.

[17] A. Quarteroni, R. Sacco, F. Saleri, Numerical Mathematics, 2007.

[18] S. Børresen, Spent fuel analyses based on in-core fuel management calculations, in: Proc. of PHYSOR 2004, the Physics of Fuel Cycles and Advanced Nuclear Systems: Global Developments, Chicago, Illinois, April 25–29, 2004.

[19] R.J.J. Stamm'ler, M.J. Abbate, Methods of Steady-State Reactor Physics in Nuclear Design, Academic Press, 1983, p. 384.

[20] Y. Nakahara, K. Suyama, J. Inagawa, R. Nagaishi, S. Kurosawa, N. Kohno, M. Onuki, H. Mochizuki, Nuclide composition benchmark dataset for verifying burnup codes on spent light water reactor fuels, Nucl. Technol. 137 (2) (2002) 111–126, https://doi.org/10.13182/NT02-2.

[21] N. Soppera, M. Bossant, E. Dupont, JANIS 4: an improved version of the NEA java-based nuclear data information system, Nucl. Data Sheets 120 (2014) 294–296.

[22] O. Leray, D. Rochman, P. Grimm, H. Ferroukhi, A. Vasiliev, M. Hursin, G. Perret, A. Pautz, Nuclear data uncertainty propagation on spent fuel nuclide compositions, Ann. Nucl. Energy 94 (2016) 603–611, https://doi.org/10.1016/j.anucene.2016.03.023.

[23] Guide for Validation of Nuclear Criticality Safety Calculational Methodology, U.S. National Regulatory Commission, 2001. NUREG/CR-6698.

[24] Curve Fitting Toolbox User's Guide, MathWorks, Inc., July 2001.

[25] Isotopic Analysis of High-Burnup PWR Spent Fuel Samples from the Takahama-3 Reactor, NUREG/CR-6798, ORNL/TM-2001/259, Oak Ridge National Laboratory, U.S. Nuclear Regulatory Commission Office of Nuclear Regulatory Research Washington, DC 20555-0001.

[26] S. M. Bowman, M. E. Dunn, D. F. Hollenbach, W. C. Jordan, SCALE Cross-Section Libraries, Vol. III, Sect. M4 in SCALE: A Modular Code System for Performing Standardized Computer Analyses for Licensing Evaluations, ORNL/TM-2005/39, Version 5.1, Vols. I–III, November 2006. Available from: Radiation Safety Information Computational Center at Oak Ridge National Laboratory as CCC-732.

[27] IAEA, Nuclear energy series, No.NF-T-3.8, impact of high burnup uranium oxide and mixed uranium–plutonium oxide water reactor fuel on spent fuel management. https://www.iaea.org/publications/8428/impact-of-high-burnup-uranium-oxide-and-mixed-uranium-plutonium-oxide-water-reactor-fuel-on-spent-fuel-management.